AD_____

Award Number: DAMD17-02-1-0378

TITLE: The Role of GADD34 (Growth Arrest and DNA Damage-Inducible Protein) in Regulating Apoptosis, Proliferation, and Protein Synthesis in Human Breast Cancer Cells

PRINCIPAL INVESTIGATOR: Douglas C. Weiser

CONTRACTING ORGANIZATION: Duke University Medical Center
Durham, NC 27710

REPORT DATE: July 2005

TYPE OF REPORT: Annual Summary

PREPARED FOR: U.S. Army Medical Research and Materiel Command
Fort Detrick, Maryland 21702-5012

DISTRIBUTION STATEMENT: Approved for Public Release;
Distribution Unlimited

REPORT DOCUMENTATION PAGE

Form Approved
OMB No. 0704-0188

1. REPORT DATE *(DD-MM-YYYY)*	2. REPORT TYPE	3. DATES COVERED *(From - To)*
01-07-2005	Annual Summary	1 Jul 2002 – 30 Jun 2005

4. TITLE AND SUBTITLE
The Role of GADD34 (Growth Arrest and DNA Damage-Inducible Protein) in Regulating Apoptosis, Proliferation, and Protein Synthesis in Human Breast Cancer Cells

5a. CONTRACT NUMBER

5b. GRANT NUMBER
DAMD17-02-1-0378

5c. PROGRAM ELEMENT NUMBER

6. AUTHOR(S)
Douglas C. Weiser

E-mail: dcweiser@duke.edu

5d. PROJECT NUMBER

5e. TASK NUMBER

5f. WORK UNIT NUMBER

7. PERFORMING ORGANIZATION NAME(S) AND ADDRESS(ES)
Duke University Medical Center
Durham, NC 27710

8. PERFORMING ORGANIZATION REPORT NUMBER

9. SPONSORING / MONITORING AGENCY NAME(S) AND ADDRESS(ES)
U.S. Army Medical Research and Materiel Command
Fort Detrick, Maryland 21702-5012

10. SPONSOR/MONITOR'S ACRONYM(S)

11. SPONSOR/MONITOR'S REPORT NUMBER(S)

12. DISTRIBUTION / AVAILABILITY STATEMENT
Approved for Public Release; Distribution Unlimited

13. SUPPLEMENTARY NOTES

14. ABSTRACT
GADD34 is a stress-induced proteins implicated in the control of protein synthesis and apoptosis. It is a major target of the oncogene c-myc. Myc is widely implicated in breast cancer and potently inhibits GADD34 expression. The goal of this proposal is to better understand the mechanism of GADD34 induced apoptosis and the implications of this to human breast cancer. Toward this goal we have analyzed the regulation of eIF2 alpha dephosphorylation by GADD34 and by its binding partner Inhibitor-1. We have demonstrated that proper subcellular localization of GADD34 is necessary for function. We have identified a novel domain that targets GADD34 to the endoplasmic reticulum, and a domain involved in PP1 binding. We also examined the role of I-1, a GADD34 interacting protein that inhibits PP1, in inhibiting eIF2 alpha dephosphorylation and identified a novel domain necessary for the *in vivo* function of I-1. We also demonstrated that this domain is absent in 2 alternate splice forms of I-1, I-1 alpha and I-1 beta, which are weaker inhibitors of eIF2 alpha dephosphorylation. We have also demonstrated that GADD34 protein levels are elevated in human cancer cells in response to a variety of stressed. Interestingly, p38 MAP kinase is required for GADD34 induction by aresnite, but not endoplasmic-reticulum stress. GADD34 is also a rapidly degraded protein,consistent with a temporal regulation of stress-signaling. This work has lead to a better understanding of GADD34 function in cancer cell, and may lead to better anti-breast-cancer drugs targeting this apoptotic pathway.

15. SUBJECT TERMS
GADD34, eIF2 alpha, I-1, PP1, Myc, Translation, Apoptosis

16. SECURITY CLASSIFICATION OF:			17. LIMITATION OF ABSTRACT	18. NUMBER OF PAGES	19a. NAME OF RESPONSIBLE PERSON
a. REPORT	b. ABSTRACT	c. THIS PAGE			19b. TELEPHONE NUMBER *(include area code)*
U	U	U	UU	29	

Table of Contents

Introduction

The proto-oncogene c-myc has been widely implicated in human cancer[1]. One of the major cellular targets of c-myc is the stress-induced gene GADD34. GADD34 is a potent apoptotic-inducer, but c-myc expression potently inhibits GADD34 expression, indicating that GADD34 may be an important target of c-myc-mediated oncogenesis[2]. GADD34 is a scaffolding protein that interacts with several proteins including Protein Phosphatase 1 (PP1) and a PP1 inhibitor, Inhibitor-1 (I-1)[3]. GADD34 binds and targets PP1 to the eukaryotic initation factor 2 alpha (eIF2 alpha) and promotes its dephosphorylation. The reversible phosphorylation of eIF2 alpha is a critical step in the control of translation by stress signaling and is the target of several kinases. Interestingly, the anti-cancer drug methylselenocysteine (MSC or Avemar) both promotes apoptosis and GADD34 expression in human cancer cells[4]. Another drug, salubrinal, inhibits the GADD34-PP1 complex, and inhibits apoptosis in mammalian cells[5]. This indicates that GADD34 could prove to be an important target for anticancer therapies.

Body:

I proposed to study the mechanism of action of GADD34 in stress signaling, translational control and apoptosis. A better understanding of the molecular mechanism of GADD34 could lead to new avenues of research into anti-cancer therapy. During the first year of this project I began generating GADD34-specific antibodies. I also performed a systematic deletion and mutatgenesis experiment with human GADD34 to determine the domains required for stress-signaling and apoptosis. I identified an N-terminal domain required for proper subcellular localization of GADD34 and a bipartite C-terminal domain required for PP1 binding. This domain consists of a canonical RVXF, PP1-binding motif and a novel Arg-Ala rich domain, both of which were required for PP1 binding. This work was published[6] and reported in previous annual summaries.

In the second year of study, I undertook experiments in to the regulation of eIF2a dephosphorylation by inhibitor-1 a GADD34 binding protein. Expression of I-1 in human cell lines or heterologus expression in yeast, results in increased eIF2 alpha phosphorylation, indicating an inhibition of PP1-mediated eIF2alpha dephosphorylation. To better understand the mechanism of I-1 action, I performed systematic deletion analysis and identified a novel C-terminal domain of I-1, which is required for full inhibition of PP1 function in cells. Interestingly, this domain is deleted in two alternate splice forms of I-1, I-1 alpha and I-1 beta, both of which are weaker inhibitors of PP1 than I-1. This work was published[7] in the third year of the project and is attached (appendix 1) and listed as reportable outcomes.

Key Research Accomplishments:

In the thirds year of study, I collaborated with other members of the lab and generated mutant forms of PP1 missing important surface residues involved in recognizing PP1-targeting proteins, including GADD34 and I-1. We identified several residues of PP1 involved in the specificity of interaction with PP1-targets. See the attached manuscript for a more detailed analysis of the data[8]. Also, I undertook a

collaboration not directly related to this fellowship, involving the regulation of cardiac physiology by PP1 and I-1[9].

Finally, in the third year of the fellowship I wrote and defended my thesis, "Regulation of Protein Phosphatase 1" My thesis included the experiments involved in this proposal as well as additional work into PP1 function. In my thesis, I focused on the PP1-targeting subunit, GADD34 (Growth Arrest and DNA Damage Inducible Gene 34), and the PP1-inhibitory subunit, Inhibitor-1 (I-1). GADD34 and I-1 form a trimeric complex with PP1, the first example of this mechanism of PP1 regulation. This led us to examine other examples of multimeric PP1 complexes, including the neurabin-PP1-I-2 complex and CDC25-PP1-14-3-3 complex.

I divided my thesis into 7 chapters. This first chapter describes the background and importance of reversible protein phosphorylation. Specifically, it focused on the regulation of protein dephosphorylation with emphasis on the control of translation initiation by reversible protein phosphorylation. Chapter 2 contains the methods used in the study. Chapter 3 examines the role of GADD34 in the regulation of protein synthesis and PP1[6]. Chapter 4 is a characterization of the trimeric GADD34-PP1-I-1 complex[3]. Chapter 5 details my work with I-1 which established that three domains of I-1 interact with PP1 and that I-1 specifically regulates eIF2alpha dephosphorylation[7]. Chapter 6 is an examination of another multimeric PP1 complex, Neurabin-PP1-I-2[10]. Chapter 7 explores future directions for this research. The Appendices discuss collaborative projects I engaged in, including the identification of a CDC25-PP1-14-3-3 complex that regulates entry into mitosis[11] and an analysis of the importance of I-1 in control phospholamban dephosphorylation which regulates cardiac contractility[9].

The work in my thesis played an important part in the understanding of phosphatase regulation by multimeric complex. The GADD34 I-1, PP1 complex was the first complex of multiple PP1 regulators to be studied. Since, this work multiple such complexes have been identified and has led to a better understanding of the combinatorial control of PP1. Also, my work helped elucidate the regulation translation by stress-signaling by elucidating the mechanism of PP1 regulation by GADD34 and I-1.

Reportable Outcomes:

The following publications were published between July 2004-July 2005 (note: Weiser et al., 2004 was listed in the 2004 annual summary as in press):

Jennifer B. Gibbons, **Douglas C. Weiser**, Shirish Shenolikar. "Importance of a Surface Hydrophobic Pocket on Protein Phosphatase-1 Catalytic Subunit in Recognizing Cellular Regulators". (2004) *Journal of Biological Chemistry.* (2005) 280:15903-11. (appendix 2)

Anand Pathak, Federica del Monte, Wen Zhao, Jo-El Schultz, John N. Lorenz, Ilona Bodi1, **Douglas C. Weiser**, Harvey Hahn, Andrew Carr, Faisal Syed, Nirmala Mavila, Leena Jha, Jiang Qian, Yehia Marreez, Guoli Chen, Dennis W. McGraw, E. Kevin Heist, J. Luis Guerrero, Anna A. DePaoli-Roach, Roger J. Hajjar and Evangelia G. Kranias. "Enhancement of Cardiac Function and Suppression of Heart Failure Progression by Inhibition of Protein Phosphatase 1". *Circulation Research* (2005) 96:756-66.

Douglas C. Weiser, Suzanne Sikes, Shi Li, Shirish Shenolikar. "The Inhibitor-1 C-Terminus Facilitates Hormonal Regulation of Cellular Protein Phosphatase-1: Functional Implications for Inhibitor-1 Isoforms". (2004) *Journal of Biological Chemistry.* 279:48904-14. (appendix 1)

The following meeting posters were presented:
Regulation of Stress Response Signaling by Inhibition of Eukaryotic Initiation Factor 2 alpha Phosphatase Activity. **Douglas C Weiser**. American Society for Cell Biology Meeting, Washington D.C., Dec 2004.

Regulation of the Dephosphorylation of eIF2 alpha by Inhibitor-1. **Douglas C Weiser**, Shirish Shenolikar. Department of Pharmacology and Cancer Biology Retreat, Sept, 2004.

The following thesis was written:
"Regulation of Protein Phosphatase 1", **Douglas C Weiser**, 2004, Ph.D. Duke Univeristy

Conclusions:

GADD34 is a stress-regulated protein involved in the control of translation and apoptosis during stress signaling. In the tree years of this fellowship, I examined the role of GADD34 in stress signaling, demonstrating that PP1 binding, allosteric regulation and subcelllar targeting were required for GADD34 function. I also examined the GADD34-binding protein I-1 and its role in eIF2alpah dephosphorylation. I demonstrated that I-1 inhibits PP1-mediated eIF2alpha dephosphoryaltion in a variety of systems, and that multiple domains of I-1 are required for *in vivo* activity. I also examined the structure-function of the PP1 catalytic subunit, I examined the role of several surface residues of PP1 in the specificity of interactions with targeting and inhibitory usubunits, including GADD34 and I-1. Finally, the training oportunites made ossible by this fellowship allowed me to present a poster at the ASCB meeting and successfully defend my thesis in Dec 2004.

References:

1. Secombe, J., Pierce, S. B. & Eisenman, R. N. Myc: a weapon of mass destruction. *Cell* **117**, 153-6 (2004).
2. Amundson, S. A., Zhan, Q., Penn, L. Z. & Fornace, A. J., Jr. Myc suppresses induction of the growth arrest genes gadd34, gadd45, and gadd153 by DNA-damaging agents. *Oncogene* **17**, 2149-54 (1998).
3. Connor, J. H., Weiser, D. C., Li, S., Hallenbeck, J. M. & Shenolikar, S. Growth arrest and DNA damage-inducible protein GADD34 assembles a novel signaling complex containing protein phosphatase 1 and inhibitor 1. *Mol Cell Biol* **21**, 6841-50 (2001).
4. Sinha, R. et al. Effects of methylselenocysteine on PKC activity, cdk2 phosphorylation and gadd gene expression in synchronized mouse mammary epithelial tumor cells. *Cancer Lett* **146**, 135-45 (1999).

5. Boyce, M. et al. A selective inhibitor of eIF2alpha dephosphorylation protects cells from ER stress. *Science* **307**, 935-9 (2005).
6. Brush, M. H., Weiser, D. C. & Shenolikar, S. Growth arrest and DNA damage-inducible protein GADD34 targets protein phosphatase 1 alpha to the endoplasmic reticulum and promotes dephosphorylation of the alpha subunit of eukaryotic translation initiation factor 2. *Mol Cell Biol* **23**, 1292-303 (2003).
7. Weiser, D. C., Sikes, S., Li, S. & Shenolikar, S. The inhibitor-1 C terminus facilitates hormonal regulation of cellular protein phosphatase-1: functional implications for inhibitor-1 isoforms. *J Biol Chem* **279**, 48904-14 (2004).
8. Gibbons, J. A., Weiser, D. C. & Shenolikar, S. Importance of a surface hydrophobic pocket on protein phosphatase-1 catalytic subunit in recognizing cellular regulators. *J Biol Chem* **280**, 15903-11 (2005).
9. Pathak, A. et al. Enhancement of cardiac function and suppression of heart failure progression by inhibition of protein phosphatase 1. *Circ Res* **96**, 756-66 (2005).
10. Terry-Lorenzo, R. T. et al. Neurabins recruit protein phosphatase-1 and inhibitor-2 to the actin cytoskeleton. *J Biol Chem* **277**, 46535-43 (2002).
11. Margolis, S. S. et al. PP1 control of M phase entry exerted through 14-3-3-regulated Cdc25 dephosphorylation. *Embo J* **22**, 5734-45 (2003).

Appendices:

Appendix 1:
Douglas C. Weiser, Suzanne Sikes, Shi Li, Shirish Shenolikar. "The Inhibitor-1 C-Terminus Facilitates Hormonal Regulation of Cellular Protein Phosphatase-1: Functional Implications for Inhibitor-1 Isoforms". (2004) *Journal of Biological Chemistry.* 279:48904-14.

Appendix 2:
Jennifer B. Gibbons, **Douglas C. Weiser**, Shirish Shenolikar. "Importance of a Surface Hydrophobic Pocket on Protein Phosphatase-1 Catalytic Subunit in Recognizing Cellular Regulators". (2004) *Journal of Biological Chemistry.* (2005) 280:15903-11.

Appendix 3:
Anand Pathak, Federica del Monte, Wen Zhao, Jo-El Schultz, John N. Lorenz, Ilona Boda, **Doug Weiser**, Harvey Hahn, Andrew N. Carr, Faisal Syed, Nirmala Mavila, Leena Jha, Jiang Qian, Yehia Marreez, Guoli Chen, Dennis W. McGraw, E. Kevin Heist, J. Luis Guerrero, Anna A. DePaoli-Roach, Roger J. Hajjar, Evangelia G. Kranias. "Enhancement of Cardiac Function and Suppression of Heart Failure Progression By Inhibition of Protein Phosphatase 1". *Circulation Research* (2005) 96:756-66.

THE JOURNAL OF BIOLOGICAL CHEMISTRY
Vol. 279, No. 47, Issue of November 19, pp. 48904–48914, 2004
Printed in U.S.A.

The Inhibitor-1 C Terminus Facilitates Hormonal Regulation of Cellular Protein Phosphatase-1

FUNCTIONAL IMPLICATIONS FOR INHIBITOR-1 ISOFORMS*

Received for publication, April 21, 2004, and in revised form, August 31, 2004
Published, JBC Papers in Press, September 2, 2004, DOI 10.1074/jbc.M404416200

Douglas C. Weiser‡, Suzanne Sikes, Shi Li, and Shirish Shenolikar§

From the Department of Pharmacology and Cancer Biology, Duke University Medical Center, Durham, North Carolina 27710

Inhibitor-1 (I-1) is a selective inhibitor of protein phosphatase-1 (PP1) and regulates several PP1-dependent signaling pathways, including cardiac contractility and regulation of learning and memory. The human I-1 gene has been spliced to generate two alternative mRNAs, termed I-1α and I-1β, encoding polypeptides that differ from I-1 in their C-terminal sequences. Reverse transcription-PCR established that I-1α and I-1β mRNAs are expressed in a developmental and tissue-specific manner. Functional analysis of I-1 in a *Saccharomyces cerevisiae* strain dependent on human I-1 for viability established that a novel domain encompassing amino acids 77–110 is necessary for PP1 inhibition in yeast. Expression of human I-1 in *S. cerevisiae* with a partial loss-of-function eukaryotic initiation factor-2α (eIF2α) kinase (Gcn2p) mutation permitted growth during amino acid starvation, consistent with the inhibition of Glc7p/PP1, the yeast eIF2α phosphatase. In contrast, human I-1α, which lacks amino acids 83–134, and I-1 with C-terminal deletions were significantly less effective in promoting yeast growth under starvation conditions. These data suggest that C-terminal sequences of I-1 enhance regulation of the eukaryotic eIF2α phosphatase. *In vitro* studies established that C-terminal sequences, deleted in both I-1α and I-1β, enhance PP1 binding and inhibition. Expression of full-length and C-terminally truncated I-1 in HEK293T cells established the importance of the I-1 C terminus in transducing cAMP signals that promote eIF2α phosphorylation. This study demonstrates that multiple domains in I-1 target cellular PP1 complexes and establishes I-1 as a cellular regulator of eIF2α phosphorylation.

Protein phosphatase-1 (PP1)[1] is a major eukaryotic serine/threonine protein phosphatase that controls numerous physiological processes, including protein synthesis, gene expression, the cell cycle, cardiac contractility, and neuronal signaling (1). Regulation of these diverse PP1 functions in mammalian tissues is mediated by the interaction of the PP1 catalytic subunit with a number of targeting subunits and endogenous protein inhibitors (2). The prototypic mammalian PP1 regulator, Inhibitor-1 (I-1), requires phosphorylation by protein kinase A (PKA) to inhibit PP1. I-1 is widely expressed in mammalian tissues and is a critical regulator of PP1 function in many cAMP-regulated physiological processes, including cardiac contractility (3) and neuronal signaling (4). The I-1 homolog DARPP-32 (dopamine- and cAMP-regulated phosphoprotein of apparent M_r 32,000) is predominantly expressed in neurons. I-1 and DARPP-32 share extensive sequence homology within an N-terminal domain that encompasses the threonine residue phosphorylated by PKA. N-terminal fragments of I-1 and DARPP-32 including the phosphorylated threonine inhibit PP1 *in vitro* (5, 6). Such studies also highlighted a conserved tetrapeptide sequence (KIQF) that is critical for PP1 inhibition by I-1 and DARPP-32. Subsequent studies that noted the presence of homologous sequences in several PP1 regulators as well as co-crystallization of the PP1 catalytic subunit with a peptide containing an (R/K)(I/V)XF sequence established that this domain represents a conserved PP1-binding motif found in many PP1 regulators (7).

Although the N-terminal PP1 inhibitory domains of DARPP-32 and I-1 are nearly identical, the C-terminal sequences are highly divergent, and the precise role of these sequences is largely unknown. Both I-1 and DARPP-32 are phosphorylated at serine residues in their C-terminal domains, and studies of DARPP-32 have provided the clearest insights into the function of these covalent modifications. Serine phosphorylation of DARPP-32 by casein kinases I and II modulates the phosphorylation and dephosphorylation of DARPP-32 at Thr^{34} and thereby regulates DARPP-32 function as a PP1 inhibitor (8, 9). In contrast, our studies of I-1 showed that the C terminus plays an important role in binding other cellular proteins, specifically GADD34, a scaffolding protein that also binds PP1; this generates a heterotrimeric complex with eukaryotic initiation factor-2α (eIF2α) phosphatase activity (10). We speculated that the C terminus targets I-1 to specific cellular PP1 complexes, such as GADD34·PP1, and that, following PKA phosphorylation, I-1 inhibits eIF2α phosphatase activity. In this manner, the GADD34·PP1·I-1 complex represents a mechanism by which cAMP could regulate mammalian protein synthesis.

The human I-1 gene is alternatively spliced to generate two additional mRNAs, termed I-1α and I-1β (11). Full-length I-1 differs from the I-1α and I-1β polypeptides in their C-terminal sequences. I-1α contains a deletion of amino acids 83–134, whereas I-1β results from a frameshift at amino acid 61 and

* This work was supported in part by National Institutes of Health Grant RO1-DK52054 (to S. S.). The costs of publication of this article were defrayed in part by the payment of page charges. This article must therefore be hereby marked "*advertisement*" in accordance with 18 U.S.C. Section 1734 solely to indicate this fact.

‡ Supported by Predoctoral Fellowship DAMD17-02-1-0378 from the United States Department of Defense Breast Cancer Program.

§ To whom correspondence should be addressed: Dept. of Pharmacology and Cancer Biology, Duke University Medical Center, LSRC C315, Research Dr., Durham, NC 27710. Tel.: 919-681-6178/9; Fax: 919-681-9567; E-mail: sheno001@mc.duke.edu.

[1] The abbreviations used are: PP1, protein phosphatase-1; I-1, Inhibitor-1; hI-1, human Inhibitor-1; PKA, protein kinase A; eIF2α, eukaryotic initiation factor-2α; WT, wild-type; 3-AT, 3-aminotriazole; GST, glutathione *S*-transferase; RT, reverse transcription; P, postnatal day; G_M, glycogen targeting subunit from skeletal muscle.

possesses a unique C terminus. Until this work, the functions of these novel I-1 isoforms as PP1 inhibitors, specifically the holoenzymes found in eukaryotic cells, have not been analyzed.

Biochemical studies show that human I-1 inhibits the yeast PP1 catalytic subunit, Glc7p, in an indistinguishable manner from human PP1 (12) and that expression of I-1 impacts only select PP1-dependent signaling pathways (13). Moreover, in *Saccharomyces cerevisiae* strain JC1007-97, expression of active human I-1 is essential for growth and viability (13). This provides a novel cell-based assay for examining the structure-function of I-1 as a regulator of PP1 holoenzymes. Our work validates the use of yeast as a model eukaryotic system for analyzing the function of human I-1 and shows, for the first time, that selected C-terminal residues in human I-1 are required for effective PP1 inhibition in yeast. Analysis of tissues from wild-type (WT) I-1 and I-1-null mice established that three distinct mRNAs are transcribed from a single mouse I-1 gene and confirmed that alternative splicing yields the two additional transcripts, I-1α and I-1β, in many mouse tissues. Utilizing *S. cerevisiae* strain Y27, in which Glc7p was previously shown to dephosphorylate eIF2α to allow the recovery of yeast from amino acid starvation (14), we established that human I-1α, which lacks C-terminal residues present in full-length I-1, is a less effective inhibitor of phosphatase activity. *In vitro* biochemical experiments demonstrated that the C-terminal region of I-1 enhances binding to the PP1 catalytic subunit and inhibition of phosphatase activity. Expression of I-1 in HEK293T cells demonstrated that the I-1 C terminus facilitated cAMP signals that inhibit protein translation in mammalian cells and suggested distinct roles for the newly defined isoforms, I-1α and I-1β, in regulating cellular PP1 activity.

MATERIALS AND METHODS

Antibodies—Anti-PP1 monoclonal antibody (1:1000 dilution) was obtained from BD Biosciences. Anti-I-1 (1:1000) and anti-I-1(T35-P) (1:2000) polyclonal antibodies were generated in this laboratory and used as described previously (10). Anti-eIF2α polyclonal antibody (1:500) was from Santa Cruz Biotechnology Inc. Anti-phospho-Ser^{51} eIF2α antibody (1:1000) was from BIOSOURCE. Anti-FLAG monoclonal antibody (1:1000) was obtained from Sigma.

Yeast Strains—The following yeast strains were used in this work: Y27, *MATα gcn2-507 ura3-52 leu2-3 leu2-112 ino1 HIS4-lacZ*; H1402, *MATα ura3-52 leu2-3 leu2-112 ino1 HIS4-lacZ*; H1149, *MATα gcn2::LEU2 ura3-52 leu2-3 leu2-112 ino1 HIS4-lacZ*; and JC1007-97, *MATα gfa1-97 ade2 ade3 leu2 ura3 lys2 can1*.

Human I-1 Expression Plasmids—All plasmids used in this study are listed in Table I. Deletions of human I-1 were generated using JZ205 as template. With the QuikChange site-directed mutagenesis kit (Stratagene), stop codons were added at amino acids 142, 123, 97, 77, and 54 of human I-1 (hI-1). The region encoding C-terminal amino acids 81–171 was excised from pGEM3ZF/I-1 using SacI and HindIII and ligated into pGEX-4T using EcoRI and XhoI. The N-terminal region of I-1 cDNA (encoding amino acids 1–80) was excised from pGEM3ZF/I-1 using NcoI and SacI and ligated into pRSET-B, which was then digested with BglII and SalI, and the resulting cDNA was inserted into pGEX-4T using BamHI and SalI. Expression constructs for I-1α were generated from the hI-1 cDNA by introducing NheI sites at codons 83 and 134. Following digestion with NheI, the cDNA was religated to produce a cDNA encoding hI-1α with one exception, with an alanine substitution at residue 84. Mammalian expression plasmids were generated using PCR primers that added BglII and SalI restriction sites to the hI-1 cDNA. The PCR product was digested with BglII and SalI and ligated into pCMV-FLAG-2 (Sigma) digested with BamHI and SalI. All cDNAs were confirmed by sequencing at the Duke Comprehensive Cancer Center DNA Sequencing Facility.

Yeast Assay for Amino Acid Starvation—The ability of hI-1 to suppress the phenotype of the *gcn2-507* allele was assayed as described (14, 15). Briefly, strains Y27, H1402, and H1149 were transformed with plasmids expressing hI-1 or dominant-negative *GLC7*. Cultures were grown at 30 °C on synthetic medium lacking uracil and histidine and containing 40 mM leucine and 30 mM 3-aminotriazole (3-AT) or on control medium lacking uracil. Growth was monitored as formation of yeast colonies.

TABLE I
Plasmids used in this work

Name	Description	Source/Ref.
p2168	2μ *URA3 GLC7-(1–207)*	13
pJZ203	2μ *ADE3 LEU2* Gpd1p·hI-1	13
pJZ205	CEN *URA3* Gpd1p·hI-1	13
pJZ206	2μ *URA3* Gpd1p·hI-1	13
pJZ208	CEN *URA3* Gpd1p·hI-1(T35A)	13
pRS426	2μ *URA3*	13
pSE1	pGEX-2T hI-1	5
YEp195	2μ *URA3*	13
YCp33	CEN *URA3*	13
pDW1	CEN *URA3* hI-1(F12A)	This study
pDW2	CEN *URA3* hI-1(T35D)	This study
pDW3	CEN *URA3* hI-1-(1–142)	This study
pDW4	CEN *URA3* hI-1-(1–142)(T35A)	This study
pDW5	CEN *URA3* hI-1-(1–142)(T35D)	This study
pDW6	CEN *URA3* hI-1-(1–123)	This study
pDW7	CEN *URA3* hI-1-(1–123)(T35A)	This study
pDW8	CEN *URA3* hI-1-(1–123)(T35D)	This study
pDW9	CEN *URA3* hI-1-(1–97)	This study
pDW10	CEN *URA3* hI-1-(1–97)(T35A)	This study
pDW11	CEN *URA3* hI-1-(1–97)(T35D)	This study
pDW12	CEN *URA3* hI-1-(1–77)	This study
pDW13	CEN *URA3* hI-1-(1–77)(T35A)	This study
pDW14	CEN *URA3* hI-1-(1–77)(T35D)	This study
pDW15	CEN *URA3* hI-1-(1–54)	This study
pDW16	CEN *URA3* hI-1-(1–54)(T35A)	This study
pDW17	CEN *URA3* hI-1-(1–54)(T35D)	This study
pDW18	CEN *URA3* hI-1-(Δ77–97)	This study
pDW19	CEN *URA3* hI-1-(Δ77–97)(T35A)	This study
pDW20	CEN *URA3* hI-1-(Δ77–97)(T35D)	This study
pDW21	CEN *URA3* hI-1-(Δ97–110)	This study
pDW22	CEN *URA3* hI-1-(Δ97–110)(T35A)	This study
pDW23	CEN *URA3* hI-1-(Δ97–110)(T35D)	This study
pDW24	CEN *URA3* hI-1-(Δ110–123)	This study
pDW25	CEN *URA3* hI-1-(Δ110–123)(T35A)	This study
pDW26	CEN *URA3* hI-1-(Δ110–123)(T35D)	This study
pDW27	CEN *URA3* hI-1α	This study
pDW28	2μ *URA3* hI-1(T35A)	This study
pDW29	2μ *URA3* hI-1-(1–77)	This study
pDW30	pGEX-4T hI-1-(1–80)	This study
pDW31	pGEX-4T hI-1-(81–171)	This study
pDW32	pGEX-2T hI-1-(Δ77–110)	This study
pDW33	pGEX-2T hI-1α	This study
pDW34	pFLAG-CMV-2 hI-1	This study
pDW35	pFLAG-CMV-2 hI-1(T35A)	This study
pDW36	pFLAG-CMV-2 hI-1-(1–77)	This study

Sectoring Assay in S. cerevisiae gfa1-97—Yeast sectoring assays were performed as described (13). Briefly, the yeast strain JC1007-97 containing JZ203 was transformed with competing hI-1-expressing plasmids, and yeast cells were grown on synthetic medium lacking uracil and reduced adenine (6 μg/ml). The red-and-white sectoring colonies were counted after 4 days of growth at 30 °C. Deletions of hI-1 were generated using gap repair. PCR primers were designed that included the GDP promoter and various 5′-regions of hI-1 cDNA from JZ205. The PCR-amplified cDNAs in the linearized plasmids YEp195 (2μ *URA3*) and YCp33 (CEN *URA3*) were transformed into JC1007-97, and yeast cells were grown as described (13).

Immunoblotting of Yeast Lysates—Yeast cells were grown on nonselective medium at 30 °C to A_{600} = 0.6. The cells were centrifuged at 5000 × *g* for 5 min. The pellet was resuspended in 500 μl of ice-cold lysis buffer (50 mM Tris-HCl (pH 7.5), 150 mM NaCl, 1 mM EDTA, 1 mM EGTA, 0.1% (v/v) β-mercaptoethanol, 0.5% (w/v) Triton X-100, 1 mM benzamidine, 1 mM phenylmethylsulfonyl fluoride, 2 μg/ml leupeptin, 1 μg/ml aprotinin, and 1 μg/ml pepstatin), mixed with an equal volume of glass beads, and vortexed at full speed for five bursts of 20 s. The lysate was then cleared by centrifugation at 20,000 × *g* for 10 min. The lysate was analyzed by immunoblotting.

Expression of Recombinant hI-1—The pGEX-4T constructs encoding glutathione *S*-transferase (GST) fused to I-1-(1–171), I-1-(1–80), and I-1-(81–171) were transformed into *Escherichia coli* BL21(DE3) RIL cells, and bacteria were grown overnight in 50 ml of LB medium containing ampicillin (100 μg/ml) and chloramphenicol (33 μg/ml) at 30 °C. Cultures were grown at 30 °C to A_{600} = 0.5, cooled to 18 °C, and

induced with 0.1 mM isopropyl 1-thio-β-D-galactopyranoside for 12 h. Bacteria were sedimented by centrifugation at 3000 × *g* for 10 min and resuspended in 10 ml of ice-cold buffer containing 10 mM Tris-HCl (pH 7.5), 150 mM NaCl, 1 mM EDTA, 1 mM EGTA, 0.1% (v/v) β-mercaptoethanol, 0.1% (w/v) Triton X-100, 1 mM benzamidine, 1 mM phenylmethylsulfonyl fluoride, 2 μg/ml leupeptin, 1 μg/ml aprotinin, and 1 μg/ml pepstatin. The resuspended cultures were lysed by sonication, and cell debris was removed by centrifugation at 25,000 × *g* for 10 min.

Bacterial lysates were incubated with glutathione-Sepharose (Amersham Biosciences) for 1 h at 4 °C. Beads were rinsed three times with 50 ml each of lysis buffer, followed by 10 mM Tris-HCl (pH 7.5), 150 mM NaCl, 0.1% (v/v) β-mercaptoethanol, 1 mM EDTA, and 1 mM EGTA. GST fusion proteins were eluted with 100 mM Tris-HCl (pH 8.0), 150 mM NaCl, and 10 mM glutathione. Eluted proteins were dialyzed into 50 mM Tris-HCl (pH 7.5), 0.1% (v/v) β-mercaptoethanol, and 0.005% (w/v) Brij 35. GST-I-1α and GST-I-1-(Δ77–110) were expressed as described above, with the exception that protein induction was carried out for 3 h at 37 °C.

PP1 Sedimentation—Glutathione-Sepharose beads (25-μl bed volume) were washed twice with Tris-buffered saline (10 mM Tris-HCl (pH 7.5) and 150 mM NaCl). GST fusion proteins were incubated with washed beads in Tris-buffered saline (total volume of 300 μl) for 1 h at 4 °C. Protein-bound beads were sedimented by centrifugation at 500 × *g* and rinsed twice with Tris-buffered saline. HEK293T cell lysate (300 μg of total protein) in Tris-buffered saline, 1 mM EDTA, 1 mM EGTA, and 0.1% (w/v) Triton X-100 was incubated with the GST fusion protein-bound beads for 1 h at 4 °C. Beads were washed five times with 1 ml each of the same buffer, resuspended in SDS-PAGE sample buffer, and analyzed by SDS-PAGE. PP1 was detected by Western immunoblotting with anti-PP1 antibody. All PP1 sedimentation assays were performed three times with two independent preparations of recombinant I-1 protein.

Phosphorylase Phosphatase Assay—Phosphorylase phosphatase assays were performed in 50 mM Tris-HCl (pH 7.5), 1 mM EDTA, and 0.1% (v/v) β-mercaptoethanol with PP1 catalytic subunit (0.02 units) purified from rabbit skeletal muscle and hI-1 proteins. I-1 was phosphorylated using purified bovine cardiac PKA catalytic subunit (16). Two independent preparations of each I-1 fusion peptide were phosphorylated. The stoichiometry of phosphorylation was established by "back-phosphorylation" of all phosphorylated I-1 polypeptides using fresh PKA and [^{32}P]ATP and analysis of ^{32}P incorporation to ensure 1 mol/mol phosphorylation of all GST-I-1 proteins.

The assays were initiated by [^{32}P]phosphorylase (final concentration of 2 mg/ml), and the mixture was incubated for 30 min at 37 °C. Assays were terminated by addition of 200 μl of 20% (w/v) trichloroacetic acid and 50 μl of bovine serum albumin (10 mg/ml) and subjected to centrifugation at 15,000 × *g* for 10 min. [^{32}P]Phosphate release was analyzed by liquid scintillation counting. All assays were performed at least three times in triplicate.

Expression of I-1 in Cultured Mammalian Cells—HEK293T cells (grown to near confluency in 6-well plates) were transfected with 2.0 μg of FLAG-hI-1 DNA, 2.0 μg of FLAG-hI-1(T35A) DNA, 2.0 μg of FLAG-hI-1-(1–77) DNA, or 2.0 μg of vector control (pCMV-FLAG-2) and 4 μl of LipofectAMINE (Invitrogen) according to the manufacturer's instructions. Cells were then treated with 0.1% Me_2SO or 5 μM forskolin. After 6 h, cells were washed with phosphate-buffered saline and lysed in 500 μl of radioimmune precipitation assay buffer (10 mM sodium phosphate (pH 7.5), 150 mM NaCl, 1% (w/v) Nonidet P-40, 0.5% (w/v) deoxycholate, and 0.1% (w/v) SDS) for 15 min on ice. Cells were scraped, and the lysates were cleared by centrifugation at 20,000 × *g* for 3 min. The cleared lysates were then run on SDS-polyacrylamide gels and analyzed by immunoblotting. Immunoblots were quantified using Scion Image Beta 4.0.2. I-1 phosphorylation was normalized to total I-1 and then reported as -fold increase relative to control Me_2SO-treated cells (n = 4). Phosphorylation of eIF2α was normalized to total eIF2α and reported as -fold change relative to cells expressing the vector control (n = 4).

Reverse Transcription (RT)-PCR for I-1 mRNAs—Total cellular RNA was harvested using TRIzol (Invitrogen). mRNA was isolated from 50 μg of total RNA using Oligotex mRNA purification resin (QIAGEN Inc., Valencia, CA) and resuspended in a final volume of 40 μl. Reaction mixtures (20 μl) consisting of mRNA (10 μl), dNTPs (250 μM), oligo(dT) primers (5 pmol), dithiothreitol (8.75 mM), and RNasin (20 units; Promega) were preincubated at 75 °C for 5 min to denature RNA and cooled rapidly to 42 °C. Reverse transcription was initiated by immediate addition of Moloney murine leukemia virus reverse transcriptase (100 units; Promega). Reactions were incubated at 42 °C for 60 min and then heat-inactivated at 95 °C for 5 min. The resulting cDNAs (3 μl) were amplified with oligonucleotide primers (1 pmol) specific for I-1 (5′-ATG GAG CCC CGA CAA CAG CCC ACG-3′ (sense) and 5′-ATC CCC GGA TAC CAA CTT CTG-3′ (antisense)) or β-actin transcripts (5′-G TGG GCC GCC CTA GGC ACC AG-3′ (sense) and 5′-CTC TTT GAT GTC ACG CAC GAT TTC-3′ (antisense)). The I-1α and I-1β splice variants were selectively amplified using sense primers that spanned the alternative splice junctions (where the underlined nucleotides represent the exon 6 splice acceptor site): I-1α, 5′-GAC CAC ACC CAC CAT GAA AGA G-3′ and the I-1 antisense primer; and I-1β, 5′-TCC CCA ACT CAC TTC TCA AGA G-3′ and the I-1 antisense primer. All amplifications were conducted in 50 μl of 10 mM Tris-HCl (pH 8.3), 50 mM KCl, 2 mM $MgCl_2$, 200 μM dNTPs, and *Taq* polymerase (1 unit). Reactions to amplify I-1 and β-actin cDNAs were carried out for 24 cycles of 94 °C for 30 s, 55 °C for 30 s, and 72 °C for 45 s. Annealing temperatures for I-1α and I-1β were 58 °C for 35 cycles and 63 °C for 40 cycles, respectively. The cDNAs were separated by electrophoresis on 2% (w/v) agarose gels, transferred to ZetaProbe membrane, and hybridized to radiolabeled oligonucleotides specific for exon 4 (5′-CGG AAG AAG ATG ACA AGG ACC-3′), exon 5 (5′-GAG CCA CTG AGA GCA CAG GG-3′), exon 6 (5′-GCA GAA TCC AAC CCC AAG AC-3′), and β-actin (5′-CAG GCA TTG TGA TGG ACT C-3′).

RESULTS

Numerous PP1 complexes have been identified in eukaryotic cells and are composed of PP1 catalytic subunits associated with regulatory subunits (17). The regulatory subunits target PP1 to subcellular organelles and/or direct the dephosphorylation of selected phosphoproteins. The PP1 catalytic subunit is also inhibited by several PP1-selective inhibitor proteins, such as I-1 (18). Biochemical studies show that nanomolar concentrations of PKA-phosphorylated I-1 inhibit the PP1 catalytic subunit isolated from rabbit skeletal muscle, but are less effective in inhibiting the glycogen-bound complex composed of PP1 bound to G_M (19). Analysis of I-1-null mice suggests that I-1 preferentially regulates a subset of PP1 complexes that control vascular and cardiac muscle contractility (3) and neuronal signaling (20), whereas other PP1 functions, such as glycogen metabolism (21), are essentially unaffected in the mutant mouse. The molecular basis for I-1 selectivity for specific PP1 complexes remains unknown in part because of the lack of suitable cellular assays to investigate the structure-function of I-1 as an inhibitor of PP1 function in eukaryotic cells.

Structure-Function of I-1 in Yeast—Our previous studies showed that hI-1 potently inhibits Glc7p, the budding yeast PP1 catalytic subunit, *in vitro* (12). Moreover, the overexpression of hI-1 in yeast showed that some Glc7p-regulated pathways, such as mitosis and gene transcription, are inhibited, whereas others, such as glycogen metabolism and meiosis, are essentially unaffected (13). This raised the possibility that I-1 expression in yeast could be used to define the molecular basis by which I-1 targets cellular PP1 complexes. I-1 dependence in yeast was also used in a genetic screen to identify novel Glc7p (PP1)-regulated pathways and yielded strain JC1007-97, in which the presence of active hI-1 is required for transcription of the *GFA1* (glutamine-fructose-6-phosphate transaminase-1) gene and yeast growth (13). This provided a novel assay for evaluating the mechanism of action of I-1 as a regulator of eukaryotic PP1 complexes since only an expression vector carrying a hI-1 construct with full PP1 inhibitory activity could complement the loss of existing WT hI-1. To analyze the structure-function of I-1, yeast containing JZ203 (*ADE3* hI-1) was transformed with various I-1 constructs (pDW series). The loss of the plasmid-borne *ADE3* marker, which maintains the *gfa1-97* yeast as red colonies, occurs only when pDW plasmids express functional PP1 inhibitors, and this results in the conversion of red-to-white colonies (Fig. 1). Counting the white and/or red-and-white sectoring colonies provided a measure of relative PP1 inhibitory activity of the replacement I-1 polypeptide. In this regard, the plasmid expressing hI-1-(1–171) (JZ205) resulted in significant red-to-white conversion, with >70% white colonies. I-1(T35A), expressing full-length hI-1

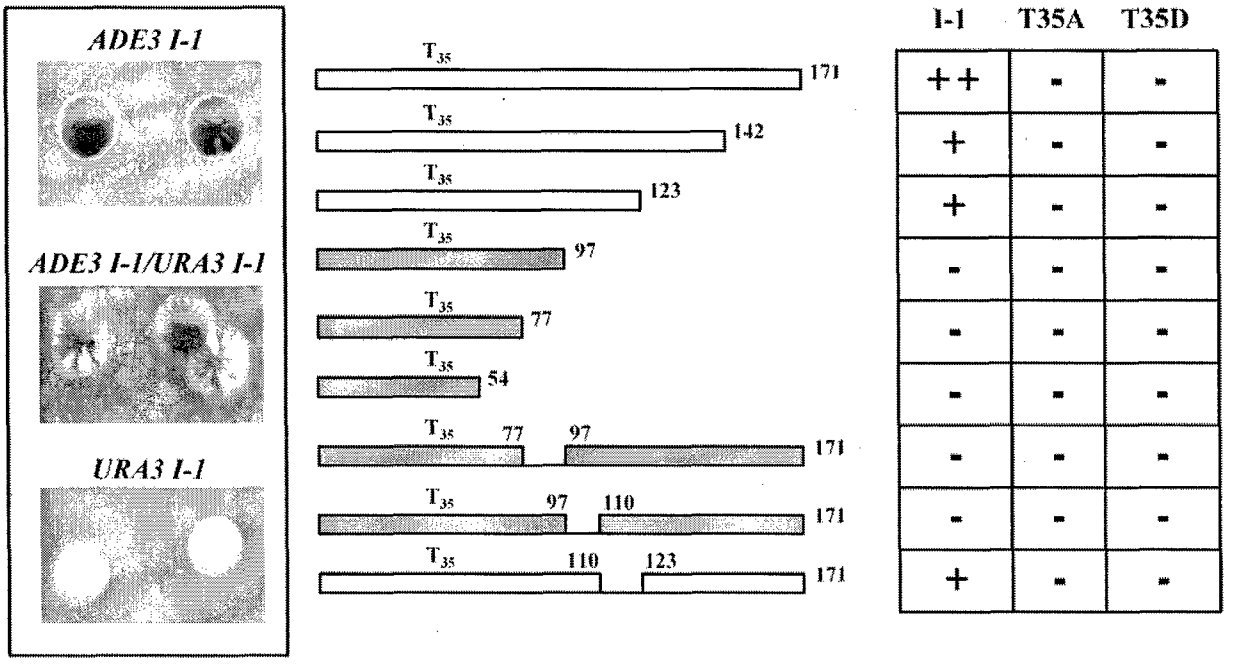

FIG. 1. **C-terminal sequences in hI-1 are required for effective PP1 inhibition in *gfa1-97* yeast.** Serial C-terminal truncations of hI-1 in *URA3* plasmids were transformed into *gfa1-97* carrying the *ADE3* hI-1 plasmid, allowing yeast growth and viability. The sectoring assay was scored for the conversion of red *ADE3* hI-1-expressing yeast to white colonies carrying *URA3* hI-1 as described under "Materials and Methods." *Left panel*, the *ADE3* I-1 plasmid (JZ203) displayed red sectors (*upper*). Yeast colonies sectoring for both *ADE3* hI-1 and *URA3* hI-1 plasmids displayed red and white sectors (*middle*). Finally, complete functional replacement of *ADE3* hI-1 yielded white colonies (*lower*). *Center panel*, the schematic shows hI-1 sequences analyzed by the yeast sectoring assay. Sequences in the plasmids that functionally complemented *ADE3* hI-1 are shown as *open bars*, whereas those lacking the ability to suppress PP1 function in *gfa1-97* are shown as *closed bars*. *Right panel*, the *table* shows the semiquantitative analysis of several independent experiments in which the individual I-1 sequences were analyzed with either Thr^{35} or substitutions T35A and T35D. Sectoring efficiency was defined as 70–100% (++), 20–70% (+), and 0–20% (−).

lacking Thr^{35}, whose phosphorylation by PKA is required for PP1 inhibition, failed to complement the loss of *ADE3* hI-1, and all colonies remained red. The C-terminal truncations I-1-(1–142) and I-1-(1–123) were also less effective inhibitors of the PP1 holoenzyme, which regulates *GFA1* transcription, and showed significantly reduced red-and-white sectoring. In contrast, I-1-(1–97), I-1-(1–77), and I-1-(1–54) failed to complement hI-1, and largely red colonies were observed, consistent with the retention of the *ADE3* hI-1 plasmid. Internal deletions that eliminated amino acids 77–97 and 97–110 also failed to complement hI-1, indicating a lack of PP1 inhibition. In contrast, hI-1 with the deletion of amino acids 110–124 was active as a PP1 inhibitor, as determined by the sectoring assay. None of the aforementioned I-1 polypeptides were functional when Thr^{35} was substituted with alanine (T35A), consistent with the absolute requirement of this phosphorylated threonine for PP1 inhibition. Interestingly, substitution of Thr^{35} with aspartic acid (T35D) to mimic threonine phosphorylation also failed to support the function of I-1 polypeptides in yeast (Fig. 1, *table*). These data suggest that, in contrast to *in vitro* studies in which PKA-phosphorylated I-1-(1–54) and I-1-(1–54)(T35D) inhibited the PP1 catalytic subunit (5), C-terminal amino acids 77–110 are required for effective inhibition of the PP1 complex(es) that regulate *GFA1* expression in the budding yeast.

In Vitro Analysis of hI-1-(Δ77–110)—To assess the functional role of the C-terminal region encompassed by amino acids 77–110, GST-I-1-(1–171) and GST-I-1-(Δ77–110) were expressed in bacteria and purified on glutathione-Sepharose. In pull-down assays with HEK293T cell lysates, stoichiometrically phosphorylated GST-I-1-(Δ77–110) sedimented significantly less PP1 than phosphorylated GST-I-1-(1–171) (Fig. 2*A*). This was particularly notable at low protein concentrations (*e.g.* 1 μg) and suggests that amino acids 77–110 facilitate I-1 binding to human PP1 complexes. Like hI-1-(1–171) (5), PKA phosphorylation of GST-I-1-(Δ77–110) also enhanced the sedimentation of purified rabbit skeletal muscle PP1 catalytic subunits, and very little PP1 bound to unphosphorylated hI-1-(1–171) (data not shown). Under identical conditions, phosphorylated GST-I-1-(Δ77–110) consistently depleted less (~22%) PP1 activity than phosphorylated GST-I-1-(1–171), which at 5 μg of total protein sedimented >50% PP1 activity (Fig. 2*B*). These data suggest that C-terminal amino acids 77–110 enhance the interaction of hI-1 with the PP1 catalytic subunit.

PKA-phosphorylated GST-I-1-(1–171) also inhibited the dephosphorylation of phosphorylase by purified PP1 catalytic subunits (IC_{50} ~ 55 nM). Phosphorylated GST-I-1-(Δ77–110) also inhibited the PP1 catalytic subunit in a dose-dependent manner in this assay (Fig. 2*C*). However, GST-I-1-(Δ77–110) showed ~10-fold reduced activity as a PP1 inhibitor compared with WT GST-I-1. Neither unphosphorylated GST-I-1-(1–171) nor unphosphorylated GST-I-1-(Δ77–110) inhibited PP1 activity at concentrations exceeding 1 μM. Differences in dose responses for GST-I-1-(1–171) and GST-I-1-(Δ77–110) were particularly notable at the higher protein concentrations (data not shown). This suggest that the N terminus of I-1 may represent a high affinity binding site for PP1 and contribute to phosphatase inhibition at low protein concentrations and that amino acids 77–110 represent a low affinity PP1-binding site that enhances PP1 binding and inhibition at higher I-1 concentrations.

Analysis of I-1 mRNAs in Mouse Tissues—Recent studies identified three hI-1 mRNAs in human brain and liver (11). In addition to the major transcript encoding full-length hI-1-(1–171), two additional mRNAs, termed I-1α and I-1β, were noted. I-1α, which lacks exon 5, was predicted to generate a shorter I-1 polypeptide (a total of 120 residues) lacking C-terminal residues 83–134. The I-1β mRNA lacks exons 4 and 5 and

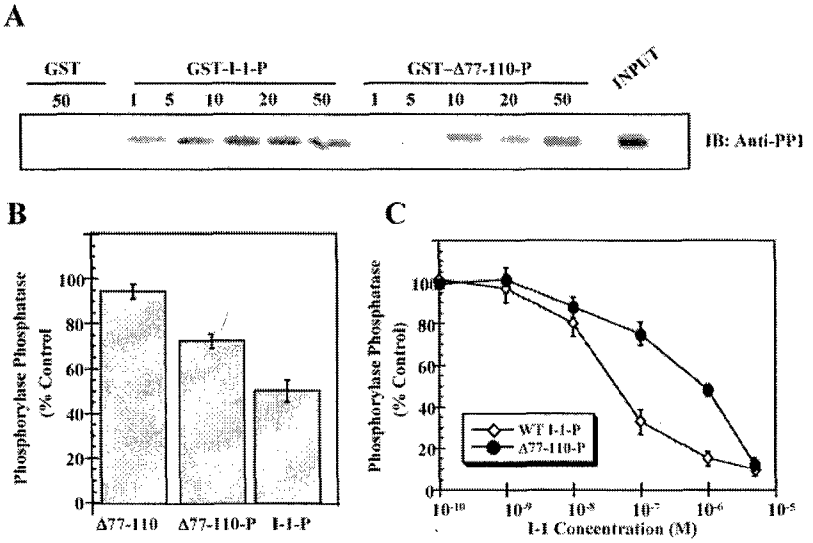

FIG. 2. **A novel C-terminal domain enhances I-1 association with PP1.** *A*, increasing amounts (micrograms of total protein) of stoichiometrically PKA-phosphorylated full-length GST-I-1 and phosphorylated GST-I-1 lacking amino acids 77–110 (*GST-Δ77–110-P*) were incubated with glutathione-Sepharose as described under "Materials and Methods" and used to sediment PP1 from HEK293T cell lysates. Bound PP1 was eluted with SDS-PAGE loading buffer and detected by immunoblotting (*IB*) with anti-PP1 antibody. The results from control pull-down assays with 50 μg of GST and input lysates (5% of the total) are also shown. *B*, 5 μg of unphosphorylated GST-I-1-(Δ77–110) (*Δ77–110*), phosphorylated GST-I-1-(Δ77–110) (*Δ77–110-P*), and phosphorylated GST-I-1 (*I–1-P*) were used to deplete purified PP1 catalytic subunits. PP1 activity remaining in solution was assayed using phosphorylase *a* as substrate. *C*, increasing concentrations of WT I-1-P (◇) and phosphorylated GST-I-1-(Δ77–110) (●) were used to inhibit the purified PP1 catalytic subunit using a phosphorylase phosphatase assay. *Error bars* indicate S.E. values for each experiment.

resulted in a frameshift, yielding a 132-amino acid polypeptide whose C terminus following amino acid 61 completely differs from those of I-1 and I-1α (Fig. 3*A*). To confirm and extend these findings, we analyzed mRNAs from tissues of WT I-1 and I-1-null mice. Oligo(dT)-primed mRNAs from mouse tissues were amplified and hybridized with probes specific for exons 4–6 (Fig. 3*B*). The specificity of these probes was established as the exon 6 probe detected all three I-1 mRNAs, the exon 5 probe detected in only I-1 mRNA, and the exon 4 probe detected in both I-1 and I-1α mRNAs. At the exposure shown in Fig. 3*B*, the mRNA levels of I-1 far exceeded those of I-1α and I-1β (which were more clearly seen at longer exposures). The signal on this Southern blot depended on the amount of mRNA analyzed (Fig. 3*B*, *lanes 28–30*). Interestingly, expression of all three mRNAs was decreased in adult testes compared with postnatal (P) days P7 and P14 and was detectable only at exposures longer than those shown in Fig. 3. Finally, the exon 6 probe showed a low signal in mouse liver, seen only by increasing the amplification cycles, as noted in rat liver (22).

Southern blotting using the exon 6 probe showed that the three I-1 mRNAs were expressed in mouse at embryonic days 9 and 15. All three mRNAs were also observed in tissues from P7, P14, and adult mice (Fig. 3*B*). Careful analysis showed that, in some tissues, *e.g.* heart, the I-1 mRNA levels were developmentally regulated, progressively decreasing from P7 to P14 to adult heart (Fig. 3*C*). Comparison of cortex and hippocampal mRNAs from WT I-1 and I-1-null mice established that all three mRNAs were derived from a single gene and were present in WT animals but absent in all tissues from I-1$^{-/-}$ mice. Amplification of β-actin confirmed that equivalent amounts of total mRNA from all tissues were analyzed.

To establish the presence of I-1α and I-1β in mouse tissues, specific PCR products were amplified using primers that spanned the splice junctions (Fig. 3*E*). This demonstrated that I-1α and I-1β mRNAs were present in all tissues, with much lower but detectable levels in testes (at P7 and P14). However, both I-1 mRNAs appeared to be absent in adult testes and liver at all stages of mouse development. In contrast to the progressive decrease in I-1 and I-1α mRNAs in heart during development, I-1β mRNA levels increased from barely detected levels in P7 heart to much higher levels in P14 and adult heart. This suggests that, although derived from a single gene, alternative splicing of I-1α and I-1β mRNAs is regulated in both a developmental and tissue-specific manner.

Regulation of Yeast Protein Translation by hI-1—Although the experiments using *S. cerevisiae* strain JC1007-97 identified a novel functional domain in the hI-1 C terminus required for Glc7p (PP1) inhibition, the biochemical pathway required for *GFA1* gene transcription and yeast growth has not been defined. Thus, the number and nature of PP1 complexes inhibited by hI-1 protein to promote *GFA1* gene expression are unknown. By comparison, numerous studies have established that both the Gcn2p protein kinase and Glc7p phosphatase control the phosphorylation state of the yeast translation initiation factor eIF2α (Sui2p). This pathway is particularly interesting because not only does it provide useful tools to study I-1 function in yeast, but PP1 regulation of eIF2α phosphorylation is also highly conserved in mammals (10, 23, 24). Under conditions of amino acid starvation, the Gcn2p kinase is activated and phosphorylates eIF2α to inhibit general protein translation and subsequently activates genes, such as that encoding the *GCN4* transcription factor, which promotes the expression of amino acid biosynthetic genes such as *HIS4* (14). The allele *gcn2-507* resulted in a partial loss-of-function Gcn2p and reduced eIF2α kinase activity and compromised the expression of *GCN4* and *HIS4* genes, therefore inhibiting the recovery from amino acid starvation (Fig. 4*A*). Thus, strain Y27 failed to grow on starvation medium (containing 3-AT). We anticipated that inhibition of yeast PP1 by phospho-hI-1 would enhance the function of the mutant eIF2α kinase and reinstate the growth of Y27 on starvation medium (14, 15).

The hI-1 expression plasmid (CEN I-1), like the control (CEN *URA3*), had no effect on the growth of strain H1402, which expresses wild-type Gcn2p, in the presence of 3-AT (Fig. 4*A*). In contrast, hI-1, but not the vector control, partially restored the growth of Y27, which contains a partial loss-of-function muta-

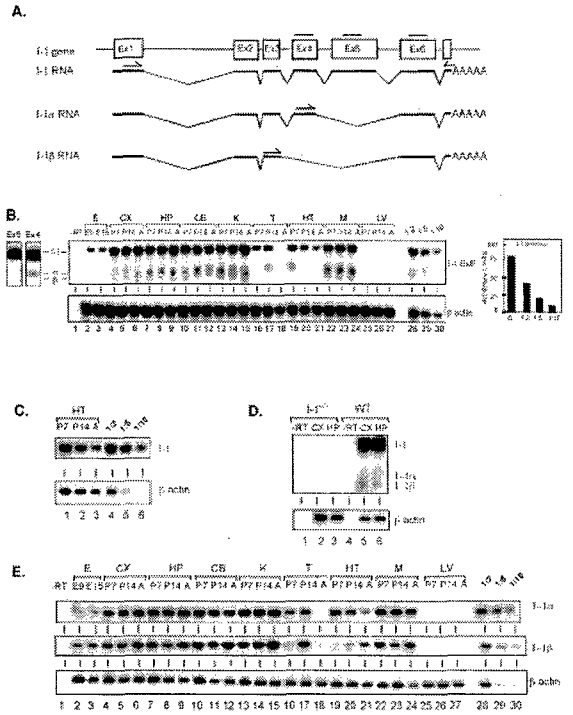

FIG. 3. **Expression of I-1 mRNAs in mouse tissues.** *A*, the schematic represents the structure of the mouse I-1 gene. Exons (*Ex*) are shown as *boxes*, and introns are shown as *lines*. The *bars* over exons 4–6 represent positions of radiolabeled exon-specific oligonucleotides described under "Materials and Methods." Alternative splicing of the I-1 gene results in I-1, I-1α, and I-1β mRNAs as shown. *Half-arrows* indicate the oligonucleotides used for splice variant-specific PCRs. *B*, semiquantitative RT-PCR was used to amplify I-1 cDNAs from total RNA harvested from mouse embryos at embryonic days 9 (*E9*) and 15 (*E15*) as well as from cerebral cortex (*CX*), hippocampus (*HP*), cerebellum (*CB*), kidney (*K*), testes (*T*), heart (*HT*), skeletal muscle (*M*), and liver (*LV*) of C57Bl/6 mice at P7, P14, and adulthood (*A*). I-1 amplification products were hybridized with oligonucleotides recognizing exon 4, 5, or 6. Amplification and hybridization with the β-actin probe established that equivalent amounts of mRNA from all mouse tissues were analyzed. Linearity of RT-PCR was established by serial dilution (*lanes 28–30*) of the cortex P7 sample. Graphical representation of I-1 titrations is shown to the right. *C*, RT-PCR showed a progressive decrease in I-1 mRNA in P7, P15, and adult heart. *D*, I-1 mRNAs were amplified from the cortex and hippocampus of WT I-1$^{+/+}$ and I-1$^{-/-}$ mice. *E*, I-1α- and I-1β-specific amplifications were undertaken using RT-PCR as described under "Materials and Methods" and hybridized with the exon 6 oligonucleotide. Amplification of β-actin mRNA established that equivalent amounts of mRNA from all mouse tissues were analyzed.

tion of *GCN2*, on starvation medium (at 30 °C for 2 days). Neither plasmid permitted the growth of H1149, in which the *GCN2* gene is disrupted, on 3-AT plates. This suggests that, by inhibiting the yeast eIF2α phosphatase (PP1), hI-1 facilitates the actions of the partially active mutant Gcn2p kinase and allows the recovery of yeast strain Y27 from amino acid starvation.

Expression of hI-1 using either low copy (CEN) or high copy (2μ) expression or expression of dominant-negative *GLC7*Δ (encoding amino acids 1–207 of Glc7p) (14) rescued Y27 growth on 3-AT plates at 30 °C for 4 days (Fig. 4*B*). Substitution of the phenylalanine in the core PP1-binding sequence (KIQF) with alanine to yield KIQA or alanine substitution of Thr^{35} (T35A) abolished I-1 function as a PP1 inhibitor. Both KIQA and T35A, like the control plasmid, failed to rescue Y27 growth on 3-AT-containing medium. Serial deletions of C-terminal sequences in hI-1 showed that I-1-(1–171), I-1-(1–142), and I-1-(1–123) allowed growth on starvation medium, but shorter I-1 polypeptides, I-1-(1–97), I-1-(1–77), and I-1-(1–54), failed to support growth on 3-AT plates (Fig. 4*C*). Yeast lysates from Y27 cells starved for 6 h were immunoblotted for phosphorylated eIF2α (Fig. 4*D*). These data show that I-1 expression in yeast resulted in increased phosphorylation of eIF2α, consistent with the inhibition of the yeast eIF2α phosphatase (Fig. 4*D*). In contrast, expression of hI-1(T35A) or the N-terminal fragment hI-1-(1–77) had no effect on I-1 phosphorylation, which essentially resembled that seen in vector control cells. These data suggest that, in addition to the KIQF PP1-binding sequence and phosphorylated threonine, C-terminal sequences between amino acids 97 and 123 are essential for inhibition of the yeast eIF2α phosphatase.

Lysates from transformed yeast cells were immunoblotted with anti-I-1 antibody to confirm equivalent expression of I-1 polypeptides (Fig. 5*A*). Expression of I-1 on a high copy plasmid (2μ) resulted in an ~10-fold higher concentration of I-1 relative to a low copy plasmid (CEN) (Fig. 5*B*). Expression of a high copy I-1 N-terminal fragment (2μ 1–77) also resulted in a 10-fold increase in expression relative to a low copy fragment (CEN 1–77) (Fig. 5*B*); however, even at this higher concentration, PP1 was insufficiently inhibited to allow Y27 growth (data not shown), indicating that truncated I-1 proteins have at least a 10-fold reduction in PP1 inhibitory activity relative to full-length I-1. Additionally, phosphorylation of hI-1 in yeast was monitored by blotting with anti-I-1(T35-P) antibody (Fig. 5*C*), confirming that N-terminal fragments of hI-1 were phosphorylated similarly to full-length hI-1, indicating that the loss of function caused by truncation of I-1 does not stem from lower expression or reduced phosphorylation, but from the reduced PP1 inhibition activity of N-terminal fragments.

Regulation of Yeast PP1 by hI-1α—Splicing of the hI-1 gene partially deleted the C-terminal domain identified in Fig. 1 to yield I-1α. To evaluate the function of I-1α as a PP1 inhibitor, hI-1α was expressed in yeast strain Y27 grown on 3-AT plates (Fig. 6*A*). Although WT hI-1 effectively promoted growth on starvation medium plates, the inactive mutant I-1(T35A) failed to facilitate yeast growth on starvation medium. Compared with hI-1, hI-1α permitted much slower growth on starvation medium. The I-1α-expressing colonies required additional 2 days (total of 6 days at 30 °C) of growth compared with hI-1-(1–171) to be visible (Fig. 6*A*). This indicates that hI-1α is a weaker PP1 inhibitor than WT hI-1 in yeast. Equal expression of I-1 peptides was confirmed by immunoblotting for I-1 (Fig. 6*A*).

For *in vitro* biochemical studies, recombinant GST-I-1α was expressed in bacteria, purified on glutathione-Sepharose, and stoichiometrically phosphorylated with PKA. In pull-down assays with HEK293T cell lysates, GST-I-1α sedimented PP1 in a dose-dependent manner. Compared with GST-I-1-(1–171), similar concentrations of GST-I-1α bound significantly less PP1 (Fig. 6*B*). This suggests that C-terminal amino acids 84–134 also facilitate I-1 association with mammalian PP1 complexes. PKA phosphorylation of GST-I-1α, as noted for hI-1, was necessary for effective sedimentation of purified PP1 catalytic subunits (Fig. 6*C*), and unphosphorylated I-1α failed to bind a significant amount of PP1 catalytic subunit.

Finally, like GST-I-1, phosphorylated GST-I-1α inhibited the phosphorylase phosphatase activity of the purified PP1 catalytic subunit (Fig. 6*D*). In this assay, I-1α showed a 3-fold reduced activity as a PP1 inhibitor. Unphosphorylated I-1α did not inhibit PP1 even at concentrations exceeding 1 μM (data not shown). These data suggest that hI-1α is a weaker PP1 inhibitor than hI-1 both *in vitro* and in yeast.

Role of the I-1 C Terminus in PP1 Binding and Inhibition—hI-1β mRNA encodes a polypeptide that shares only the N-terminal 61 amino acids with hI-1-(1–171). The frameshift introduced by excision of exons 4 and 5 incorporates an addi-

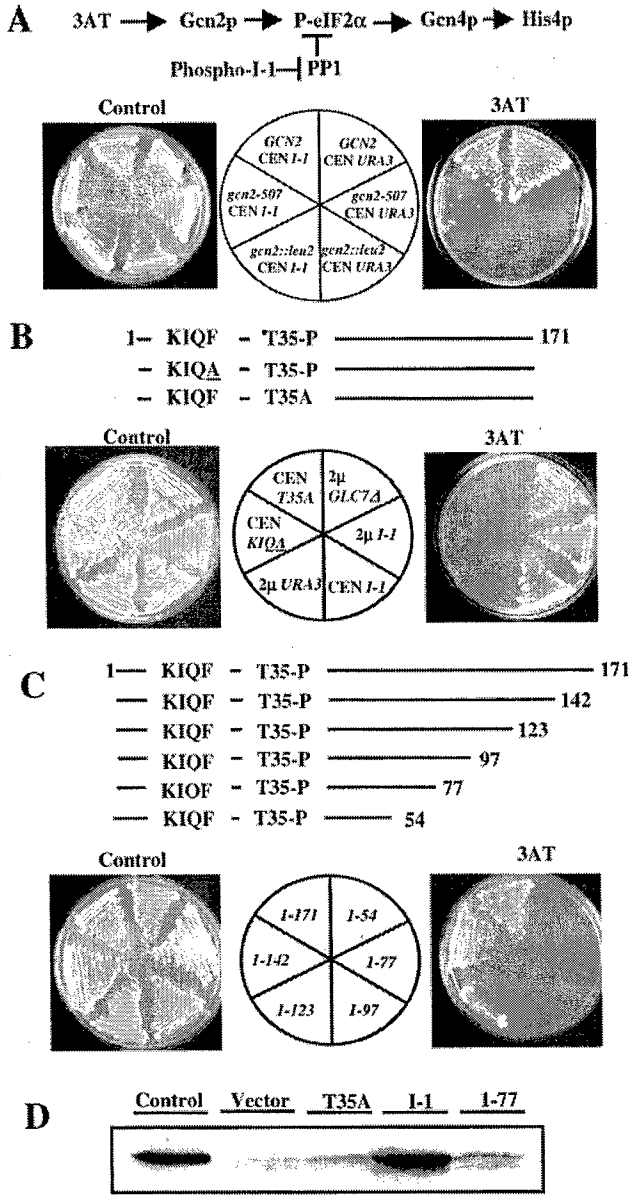

FIG. 4. **PP1 inhibition promotes growth of *gcn2-507* on starvation medium.** The ability of I-1 to inhibit Glc7p and allow the growth of *gcn2-507* yeast on starvation medium (lacking histidine and containing 3-AT) was analyzed as described under "Materials and Methods." *A*, I-1 (CEN I-1) and control CEN *URA3* were expressed in WT strains H1402 (*GCN2*), Y27 (*gcn2-507*), and H1149 (*gcn2::LEU2*); plated on either selection medium (3-AT) or control medium; and evaluated for growth for 2 days at 30 °C. *B*, the requirement for PP1 inhibition was analyzed by expression of the two inactive I-1 proteins (CEN I-1(T35A) and CEN I-1(KIQA)). The control empty vector (2μ *URA3*) was also expressed. In addition, growth in the presence of high copy (2μ hI-1) and low copy (CEN hI-1) expression was analyzed. PP1 inhibition by dominant-negative *GLC7* (2μ *GLC7*Δ) was also assessed. Transformed yeast cells were grown on starvation medium at 30 °C for 4 days. *C*, WT hI-1-(1–171) and the serial C-terminal truncations of hI-1, hI-1-(1–142), hI-1-(1–124), hI-1-(1–97), hI-1-(1–77), and hI-1-(1–54), were expressed in Y27 yeast grown on control and selection (3-AT) media. *D*, the impact of I-1 expression on eIF2α phosphorylation was directly measured using anti-phospho-Ser[51] eIF2α antibody. The vector control, I-1(T35A), WT I-1, and truncated I-1-(1–77) were expressed in strain H1402, starved, lysed, and immunoblotted (*IB*). The control was an okadaic acid-treated HEK293T cell lysate (23).

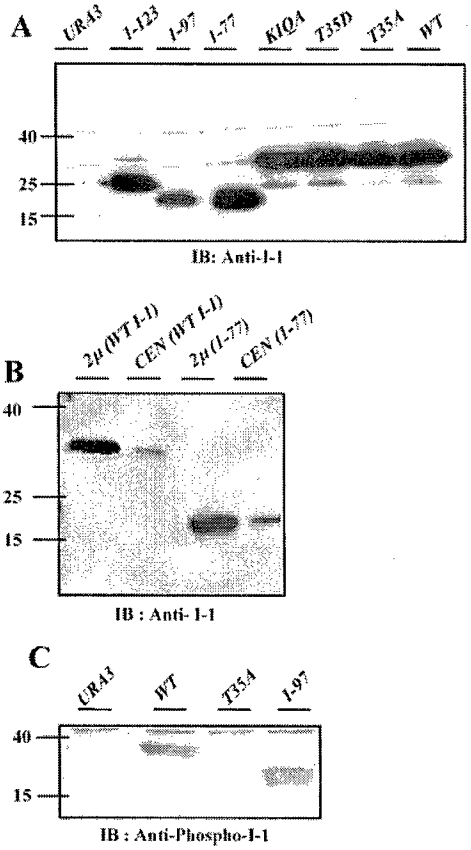

FIG. 5. **Expression and phosphorylation of hI-1 in yeast.** *A*, WT hI-1; the truncated proteins I-1-(1–123), I-1-(1–97), and I-1-(1–77); and mutants I-1(T35A), I-1(KIQA), and I-1(T35D) were expressed in Y27 yeast grown on nonselective medium. The yeast cells were lysed, and I-1 expression was analyzed by immunoblotting (*IB*). *B*, high copy (2μ) and low copy (CEN) expression of hI-1 and hI-1-(1–77) was similarly analyzed. *C*, phosphorylation at Thr[35] in full-length hI-1 and truncated hI-1-(1–97) was analyzed by immunoblotting with anti-phospho-I-1 antibody. The specificity of the phospho-specific antibody was demonstrated by the lack of cross-reactivity with lysates of Y27 cells expressing I-1(T35A).

tional 71 amino acids at the C terminus unique to I-1β. Molecular cloning and *in vitro* synthesis of a cDNA encoding I-1β has also not yet been achieved. Finally, the prior studies showed that bacterial expression of recombinant GST-I-1 polypeptides containing <80 N-terminal amino acids was extremely low. Thus, we expressed GST-I-1-(1–171), GST-I-1-(1–80), and GST-I-1-(81–171) in bacteria to evaluate the functional impact of eliminating hI-1 C-terminal sequences on I-1β. GST-I-1-(1–171) and GST-I-1-(1–80) were phosphorylated using PKA, and the phosphorylated I-1 proteins (20 μg) along with GST-I-1-(81–171) were used to sediment PP1 from HEK293T cell lysates. Unphosphorylated I-1-(1–171), I-1-(1–80), and I-1-(81–171) failed to bind PP1 (Fig. 7*A*). Under comparable conditions, phosphorylated I-1-(1–171) and I-1-(1–80) bound PP1 effectively (Fig. 7*A*). Quantitative analysis of these data showed that phosphorylated I-1-(1–80) bound PP1 less effectively than phosphorylated I-1-(1–171), a difference that was most clearly seen at 1 and 5 μg of total protein (Fig. 7*B*). This observation was confirmed using thiophosphorylated I-1 and I-1-(1–80) (data not shown). These data suggest that, whereas the C terminus of I-1 in isolation may not bind PP1, its presence increases the affinity of full-length phosphorylated I-1 for binding cellular PP1 complexes.

Consistent with previous studies (10), unphosphorylated I-1 showed weak PP1 binding. High concentrations of unphosphorylated I-1 sedimented small amounts of purified PP1 catalytic subunit (Fig. 7*C*). By contrast, unphosphorylated GST-I-1-(1–80) failed to bind PP1 even at much higher concentrations. This

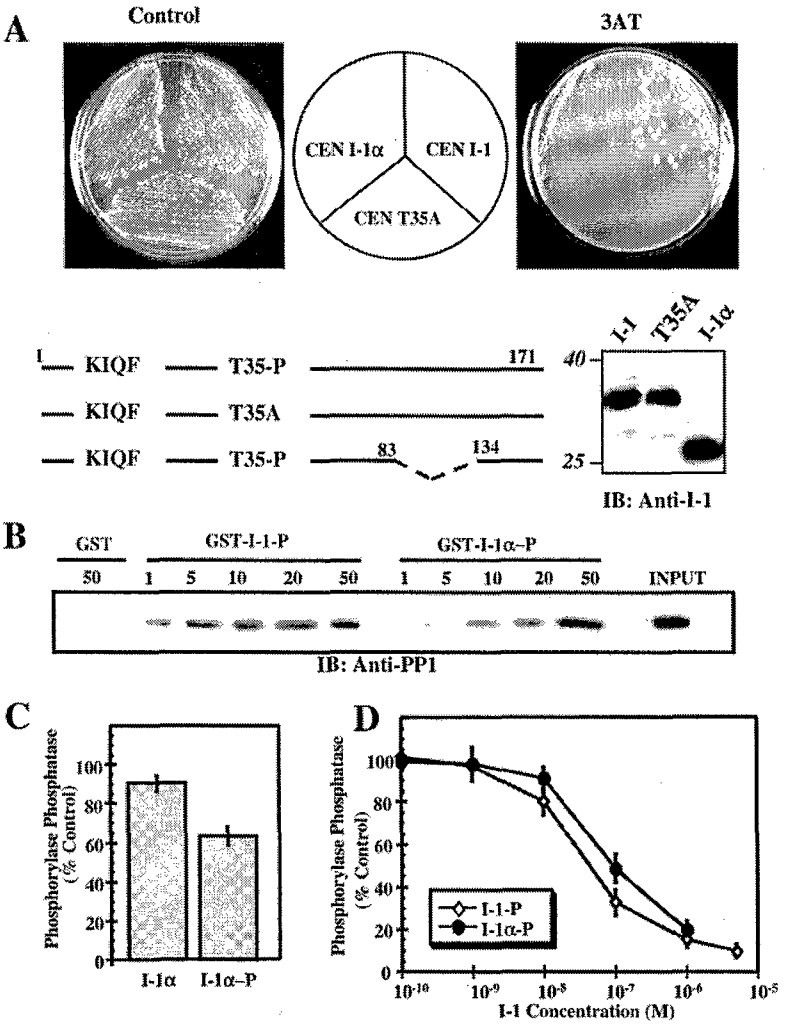

FIG. 6. **Analysis of PP1 inhibition by hI-1α.** *A*, hI-1α (CEN I-1α), I-1 (CEN I-1), and inactive I-1 (CEN I-1 T35A) were expressed in Y27 yeast and grown on control and selection (3-AT) media at 30 °C for 6 days. The schematic shows the structures of the three I-1 polypeptides analyzed. Cells were lysed and analyzed by immunoblotting (*IB*) with anti-I-1 antibody to demonstrate equal expression. *B*, phosphorylated GST-I-1 (*GST-I-1-P*), phosphorylated GST-I-1α (*GST-I-1α-P*), and GST (μg protein) were coupled to glutathione-Sepharose beads and used to sediment PP1 from HEK293T cell lysates. Bound PP1 was eluted with SDS-PAGE loading buffer and detected by immunoblotting with anti-PP1 antibody. *C*, 5 μg of phosphorylated and unphosphorylated GST-I-1α were used to deplete purified PP1 catalytic subunits from solution. Residual PP1 activity was analyzed using phosphorylase *a* as substrate. *D*, increasing concentrations of phosphorylated GST-I-1-(1–171) (◇) and phosphorylated GST-I-1α (●) were used to inhibit the PP1 catalytic subunit assayed using phosphorylase *a* as substrate. *Error bars* indicate S.E.

suggests that the C terminus of I-1 is required for low affinity PP1 binding by unphosphorylated hI-1.

In vitro phosphorylase phosphatase assays using purified rabbit skeletal muscle PP1 showed that phosphorylated GST-I-1-(1–171) and GST-I-1-(1–80) inhibited PP1 activity in a dose-dependent manner (Fig. 7*D*). Phosphorylated GST-I-1-(1–80) was nearly 10-fold weaker than phosphorylated GST-I-1-(1–171) as a PP1 inhibitor. The C-terminal fragment GST-I-1-(81–171) showed no measurable activity as a PP1 inhibitor, consistent with its inability to directly bind PP1 (data not shown). These data suggest that PP1 inhibition is mediated primarily through the N-terminal domain of I-1, which contains the PP1-binding motif KIQF and PKA-phosphorylated Thr^{35}, but that the presence of the C-terminal 90 amino acids greatly enhances the activity of I-1 as a PP1 inhibitor. In the absence of sufficient purified GST-I-1-(1–61) protein to undertake similar studies, the above data suggest that hI-1β is likely to be a weaker PP1 inhibitor than either I-1α or full-length hI-1-(1–171).

Regulation of eIF2α Dephosphorylation by I-1 in Mammalian Cells—To demonstrate the necessity of the C terminus of I-1 to regulate PP1-dependent signaling in mammalian cells, we expressed I-1 fragments in HEK293T cells, a cell line that does not express detectable I-1, and monitored the phosphorylation state of eIF2α. Expression of I-1 had little effect on eIF2α phosphorylation in untreated cells (Fig. 8*A*; quantified in Fig. 8*B*). However, when cells were treated with forskolin, which elevates intracellular cAMP, phosphorylation of I-1 and I-1-(1–77), but not I-1(T35A), was greatly increased (7.9 ± 1.6- and 5.6 ± 1.5-fold, respectively) relative to untreated I-1-expressing cells (Fig. 8*A*; quantified in Fig. 8*C*). Forskolin treatment of hI-1-expressing cells resulted in an ~70% increase in eIF2α phosphorylation. In contrast, forskolin had no effect on eIF2α phosphorylation in cells expressing either the N-terminal fragment I-1-(1–77) or the inactive mutant I-1(T35A) (Fig. 8, *A* and *B*). These data indicate that full-length I-1 is required for cAMP-induced eIF2α phosphorylation in mammalian cells and suggest that deletion of C-terminal sequences greatly impairs the ability of I-1 to inhibit the mammalian eIF2α phosphatase.

DISCUSSION

PP1, a serine/threonine protein phosphatase, is ubiquitously expressed in mammalian tissues and displays broad *in vitro* substrate specificity. In cells, however, PP1 shows considerable specificity that is dictated by the presence of >40 regulatory or targeting subunits, which direct its subcellular localization and/or substrate recognition (2). In addition, a number of PP1-specific inhibitors have been identified (18). Growing evidence suggests that, although the PP1 inhibitors potently inhibit the activity of isolated PP1 catalytic subunits, they show greater selectivity for PP1 holoenzymes containing various targeting subunits (10, 25, 26). PKA-phosphorylated I-1 inhibits the PP1 catalytic subunit with an IC_{50} of 1 nM, but even higher concentrations of phospho-I-1 have little effect of the activity of the glycogen-bound phosphatase, a complex of PP1 and G_M, the skeletal muscle glycogen-targeting subunit (19), suggesting that this complex is unlikely to be regulated by I-1 under

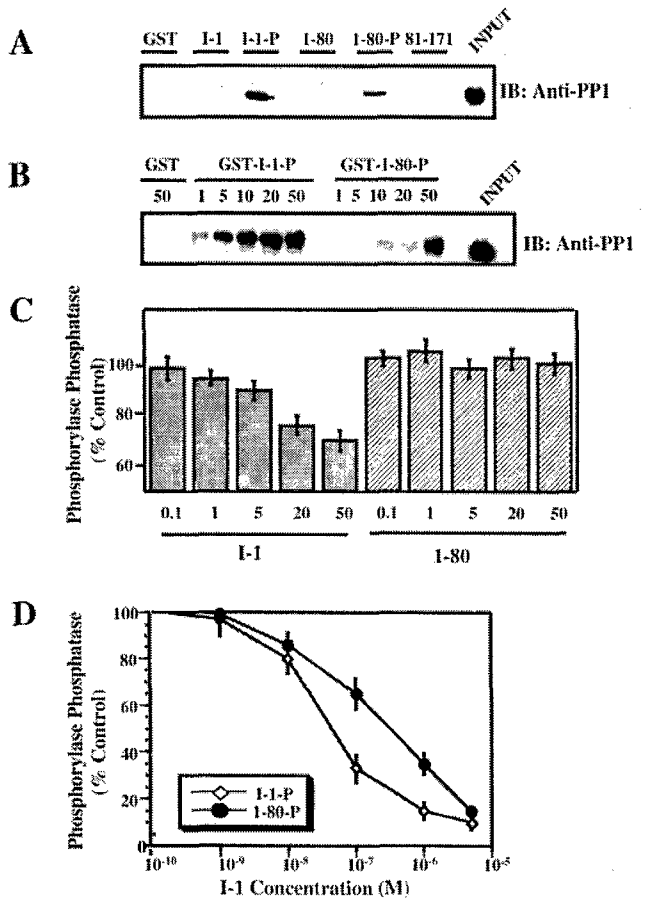

FIG. 7. **Role of the C-terminal sequences in PP1 binding and inhibition.** *A*, isolated GST, phosphorylated (*I-1-P*) and unphosphorylated (*I-1*) GST-I-1, phosphorylated (*1–80-P*) and unphosphorylated (*1–80*) GST-I-1-(1–80), and GST-I-1-(81–171) (*81–171*) were bound to glutathione-Sepharose and used to sediment PP1 from HEK293T cell lysates. Bound PP1 was eluted with SDS-PAGE sample buffer, and PP1 was detected by immunoblotting (*IB*) with anti-PP1 antibody. *B*, increasing concentrations of phosphorylated GST-I-1 and phosphorylated GST-I-1-(1–80) were used to sediment PP1 from HEK293T cell lysates, and bound PP1 was analyzed by immunoblotting with anti-PP1 antibody. *C*, increasing concentrations of unphosphorylated GST-I-1-(1–171) (*I-1*) and unphosphorylated GST-I-1-(1–80) (*1–80*) were used to deplete purified PP1 catalytic subunits from solution. Residual phosphatase activity was assayed using phosphorylase *a* as substrate. *D*, increasing concentrations of phosphorylated GST-I-1-(1–171) (*I-1-P*; ◇) and phosphorylated GST-I-1-(1–80) (*1–80-P*; ●) were used to inhibit the purified PP1 catalytic subunit analyzed as phosphorylase *a* phosphatase. *Error bars* indicate S.E.

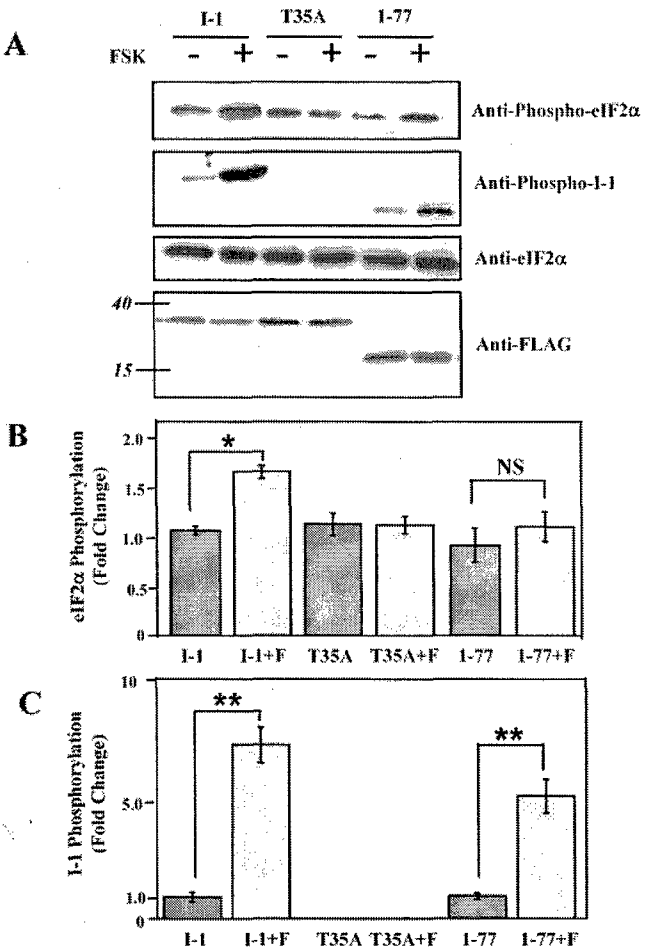

FIG. 8. **The C terminus of I-1 is required for inhibition of PP1 activity in mammalian cells.** *A*, full-length I-1, the nonfunctional mutant I-1(T35A), and an N-terminal fragment, I-1-(1–77), were expressed in HEK293T cells. Cells were treated with either 5 μM forskolin (*FSK*, *F*) for 6 h (+) or 0.1% Me_2SO (−). The cells were then lysed and immunoblotted for total protein expression (anti-FLAG antibody), phospho-I-1, total eIF2α, and phospho-eIF2α. *B*, quantification of eIF2α phosphorylation was normalized to total eIF2α content and is shown as fold change compared with cells expressing the empty vector. *, $p < 0.05$ for several independent experiments ($n = 4$) analyzed using Student's *t* test; *NS*, not significant. *C*, I-1 phosphorylation was also quantitated and normalized to total I-1 content and is shown as -fold change compared with untreated cells expressing full-length I-1. **, $p < 0.01$ for several independent experiments ($n = 4$) analyzed using Student's *t* test.

physiological conditions. In contrast, I-1 can inhibit the GADD34·PP1 complex *in vitro* with the same IC_{50} as the free catalytic subunit (10), suggesting that eIF2α phosphorylation is a potential physiological target of I-1 regulation. The PKC-activated inhibitors PHI-1 and PHI-2 (PP1 holoenzyme inhibitor) show equivalent activity *in vitro* against the PP1 catalytic subunit and the glycogen- and smooth muscle myosin-bound phosphatases (26). CPI-17, another PKC-activated PP1 inhibitor, potently inhibits the myosin-bound phosphatase, but is essentially ineffective as an inhibitor of the glycogen-bound phosphatase (27). The molecular basis by which endogenous PP1 inhibitors target some and not other PP1 complexes remains unknown.

The sequence homology between the PP1 inhibitors I-1 (a total of 171 amino acids) and DARPP-32 (a total of 204 amino acids) resides in their N-terminal 50 amino acids, which contain a conserved KIQF PP1-binding motif and the PKA-phosphorylated threonine (5, 28). The precise role of their diverse C termini is still poorly understood. *In vitro* biochemical evidence suggests that covalent modification of the unique DARPP-32 C-terminal domain allows for modulation of the phosphorylation and dephosphorylation of the critical threonine and thus fine tunes the activity of DARPP-32 as a PP1 inhibitor (8, 9, 29). In contrast, our previous work suggests that the I-1 C terminus, which is dispensable for binding to the isolated PP1 catalytic subunit *in vitro*, associates with a number of other cellular proteins, including GADD34 (10). Recent studies suggest that the specificity of some PP1 inhibitors may be dictated by their ability to bind both PP1 catalytic and targeting or regulatory subunits. Formation of such heterotrimeric complexes may dictate the specificity of CPI-17 for the myosin phosphatase (27), inhibitor-2 for the PP1·neurabin-I (25) and PP1·Nek2 complexes (30), and I-1 for the GADD34·PP1 complex (10). These studies suggest that distinct domains of these PP1 inhibitors bind the PP1 catalytic subunit and the targeting or regulatory subunit.

Recent studies suggest that alternative splicing of the hI-1

gene generates three distinct mRNAs that encode PP1 inhibitors with different C-terminal sequences (11). Alternative splicing that excises exon 5 generates I-1α, which differs from full-length I-1-(1–171) by the deletion of amino acids 83–134. Splicing of exons 4 and 5 yields I-1β, which retains the N-terminal 61 amino acids of I-1, but also has an additional 72 amino acids that share no homology with any known protein. The conservation of this splicing event was not examined. We observed the same splicing pattern in mice (Fig. 3) and cloned I-1α from a *Xenopus* embryo cDNA library.[2] As all three I-1 isoforms retain the sequences previously shown to represent the minimal PP1 inhibitory domain (11), but both splice variants lacked the novel C-terminal domain identified in our yeast experiments. The novel variants were predicted to inhibit PP1 activity, but the precise physiological role of I-1 isoforms remains unknown.

We analyzed mRNAs from tissues of WT I-1$^{+/+}$ and I-1$^{-/-}$ mice and established the presence of three distinct mRNAs encoding I-1, I-1α, and I-1β in most WT mouse tissues except liver, where very little I-1 mRNA was detected, consistent with previous studies that required extensive RT-PCR to visualize the very low levels of I-1 mRNA in rat liver (22). Previous immunoblotting studies also showed that, in contrast to other tissues, rat and mouse livers express undetectable amounts of I-1 protein (31). No I-1 mRNAs were amplified from tissues of I-1-null mice, confirming that all three mRNAs are from a single I-1 gene. Previous work showed that both I-1 mRNA (32) and protein (33) are postnatally expressed in rat brain, with low expression seen at P0, increasing thereafter to peak at P7 and finally declining to low steady-state levels in adult brain. In contrast, our studies showed a significant amount of all three I-1 mRNAs in mouse embryos at embryonic days 9 and 15. This was consistent with immunohistochemistry of whole mouse embryos that showed the presence of I-1 protein in many embryonic tissues, including high level expression in the mouse mesothelium (34). Analysis of mouse heart showed that I-1 and I-1α mRNA levels progressively decreased from P7 to adult, whereas I-1β mRNA levels increased over the same period, suggesting that I-1 mRNA expression and splicing may be regulated in both a developmental and tissue-specific manner.

In vitro structure-function studies have thus far failed to define a role of I-1 C-terminal sequences in the inhibition of the PP1 catalytic subunit (5). Thus, current studies have focused on a cell-based assay to define the functional differences between three hI-1 isoforms as PP1 inhibitors. hI-1 is phosphorylated (at Thr^{35}) when expressed in yeast (13). Moreover, hI-1 protein effectively binds and inhibits the single yeast PP1 catalytic subunit (12). Overexpression of hI-1 inhibits some PP1-regulated events while having little effect on other events (13), suggesting that hI-1 protein targets selected yeast PP1 complexes. Finally, consistent with PP1 inhibition, the functional effects of I-1 expression are suppressed by overexpression of yeast protein kinases (13). This opened the way for a novel genetic screen to identify new I-1- and PP1-regulated pathways. One such hI-1-dependent strain, JC1007-97, was used to evaluate the structural requirements for PP1 inhibition in yeast. A sectoring assay established that the phosphorylated threonine is essential for growth of *gfa1-97* suggesting a requirement for Glc7p inhibition and growth in the absence of glucosamine (13). The inactive T35A mutant failed to support *gfa1-97* growth in the sectoring assay. Surprisingly, I-1 polypeptides containing a T35D substitution to mimic phosphorylation also failed to complement the loss of WT hI-1 in *gfa1-97* yeast. Previous *in vitro* studies showed that the T35D substitution fails to activate full-length I-1 as a PP1 inhibitor (5), and deletion of the C terminus in hI-1-(1–54)(T35D) is required to inhibit PP1, albeit with a much reduced IC_{50} (~150 nM). These studies suggest a conformational cross-talk between the N- and C-terminal sequences of I-1 that is modulated by Thr^{35} phosphorylation to enhance PP1 inhibition. It should be noted, however, that the constitutively active I-1-(1–54)(T35D) peptide has been utilized to inhibit PP1 activity in mammalian cells (35) and tissues (3). Our studies suggest that high levels of expression of this weak PP1 inhibitor may overcome its reduced affinity for the PP1 catalytic subunit, and lacking C-terminal sequences that target specific PP1 complexes, the I-1-(1–54)(T35D) peptide may be more pleiotropic than WT I-1 and inhibit a wider range of PP1 complexes. Analysis of I-1 structure-function in *gfa1-97* yeast also highlighted the critical role for the I-1 C terminus, specifically amino acids 77–110, in the inhibition of the PP1 complex that activates *GFA1* gene transcription in yeast. These findings are unlikely to result from gross changes in protein folding, as previous studies used circular dichroism (5) and NMR (36) to show that I-1 is largely disordered. Yet other studies established that the PP1 inhibitory activity of I-1 is resistant to boiling and acid treatment (16). Finally, synthetic peptides derived from DARPP-32 also retain potent PP1 inhibitory activity (28). Additional biochemical studies suggest that region 77–110 stabilizes I-1 binding to the isolated PP1 catalytic subunit and selected human PP1 complexes and thereby enhances PP1 inhibition.

The biochemical pathway regulating *GFA1* gene expression has not been defined. Thus, the number and types of PP1 complexes inhibited by hI-1 in the *GFA1* pathway remain unknown. On the other hand, the ability of Glc7p to regulate protein translation in yeast has been clearly defined, and in the Y27 strain, which contains an impaired eIF2α kinase (Gcn2p), Glc7p inhibition by a truncated dominant-negative *GLC7* catalytic subunit permits yeast growth on amino acid starvation medium. hI-1 also allowed growth on starvation medium. Our results show that I-1 C-terminal sequences play a critical role in PP1 inhibition in yeast, but suggest that hI-1α, which lacks amino acids 83–134, is a weaker PP1 inhibitor. Pull-down assays with recombinant GST-I-1α also confirmed its weaker binding to human PP1 complexes from HEK293T lysates and reduced inhibition of the isolated PP1 catalytic subunit. C-terminal truncation of I-1 also suggest that I-1β, which shares only the N-terminal 61 amino acids with I-1α and I-1, is an even weaker PP1 inhibitor. These data suggest that the I-1 C-terminal sequences, while not showing direct PP1 binding, may contribute to the enhanced I-1 binding to the target phosphatase complexes.

Expression of I-1 in human HEK293T cells showed that I-1 enhanced phosphorylation of eIF2α in mammalian cells. Forskolin treatment of I-1-expressing cells activated I-1 via Thr^{35} phosphorylation and led to increased eIF2α phosphorylation. Cells expressing the inactive I-1(T35A) mutant or the vector control failed to respond to forskolin, and no significant change in eIF2α phosphorylation was observed. Interestingly, the ability of cAMP to promote eIF2α phosphorylation and thereby inhibit translation has been recognized for several decades (37). Insulin induces the simultaneous dephosphorylation of I-1 (38) and eIF2α (39), whereas hormones, such as glucagon (40) and vasopressin (41), simultaneously increase cellular cAMP and eIF2α phosphorylation. As PKA does not directly phosphorylate eIF2α or activate eIF2α kinases, the mechanism by which cAMP increases eIF2α phosphorylation remains unknown. Our studies suggest a mechanism by which hormones that increase intracellular cAMP may activate I-1 and suppress the cellular eIF2α phosphatase. As seen in yeast, deletion of

[2] S. S. Margolis and D. C. Weiser, unpublished data.

the I-1 C terminus impaired its ability to regulate protein translation. This may be consistent with our previous observation that I-1, via its C terminus, binds a key component of the mammalian eIF2α phosphatase complex, GADD34 (10). Thus, the current studies provide new evidence that the C terminus of I-1 not only enhances the affinity of I-1 for the PP1 catalytic subunit, but may also target specific PP1 complexes to regulate mammalian cell physiology. Finally, differences in PP1 binding displayed by the three I-1 isoforms, combined with predicted differences in their ability to bind specific PP1 regulatory subunits, suggest that the I-1 isoforms serve distinct roles in regulating PP1 function in mammalian cells.

In conclusion, our studies utilized novel cell-based assays in yeast and mammalian cells to highlight, for the first time, the critical role played by C-terminal sequences in regulating the potency and specificity of I-1 as a PP1 inhibitor in eukaryotic cells. Our studies provide compelling evidence for PP1 as a component of mammalian and yeast eIF2α phosphatases that are targeted by I-1 and suggest a role for I-1 in transducing the cAMP signals that inhibit protein translation in mammalian cells. Further work is clearly needed to identify additional cellular PP1 complexes targeted by I-1 and to establish the molecular basis for the immunity of other PP1 complexes to this protein inhibitor. Finally, the tissue-specific and developmental expression and the alternative splicing of the I-1 gene to generate three distinct I-1 isoforms differing in their C-terminal sequences may expand the functional diversity of this prototypic PP1 regulator.

Acknowledgments—We thank John F. Cannon, Ronald C. Wek, and Kelly Tatchell for providing reagents and advice. We also thank Susan Walsh for careful reading of the manuscript.

REFERENCES

1. Shenolikar, S. (1994) *Annu. Rev. Cell Biol.* **10,** 55–86
2. Cohen, P. T. (2002) *J. Cell Sci.* **115,** 241–256
3. Carr, A. N., Schmidt, A. G., Suzuki, Y., del Monte, F., Sato, Y., Lanner, C., Breeden, K., Jing, S. L., Allen, P. B., Greengard, P., Yatani, A., Hoit, B. D., Grupp, I. L., Hajjar, R. J., DePaoli-Roach, A. A., and Kranias, E. G. (2002) *Mol. Cell. Biol.* **22,** 4124–4135
4. Blitzer, R. D., Connor, J. H., Brown, G. P., Wong, T., Shenolikar, S., Iyengar, R., and Landau, E. M. (1998) *Science* **280,** 1940–1942
5. Endo, S., Zhou, X., Connor, J., Wang, B., and Shenolikar, S. (1996) *Biochemistry* **35,** 5220–5228
6. Desdouits, F., Cheetham, J. J., Huang, H. B., Kwon, Y. G., da Cruz e Silva, E. F., Denefle, P., Ehrlich, M. E., Nairn, A. C., Greengard, P., and Girault, J. A. (1995) *Biochem. Biophys. Res. Commun.* **206,** 652–658
7. Egloff, M. P., Johnson, D. F., Moorhead, G., Cohen, P. T., Cohen, P., and Barford, D. (1997) *EMBO J.* **16,** 1876–1887
8. Girault, J. A., Hemmings, H. C., Jr., Williams, K. R., Nairn, A. C., and Greengard, P. (1989) *J. Biol. Chem.* **264,** 21748–21759
9. Desdouits, F., Siciliano, J. C., Nairn, A. C., Greengard, P., and Girault, J. A. (1998) *Biochem. J.* **330,** 211–216
10. Connor, J. H., Weiser, D. C., Li, S., Hallenbeck, J. M., and Shenolikar, S. (2001) *Mol. Cell. Biol.* **21,** 6841–6850
11. Liu, H. T., Lin, T. H., Kuo, H. C., Chen, Y. C., Tsay, H. J., Jeng, H. H., Tsai, P. C., Shie, F. K., Chen, J. H., and Huang, H. B. (2002) *Biochem. Biophys. Res. Commun.* **291,** 1293–1296
12. Connor, J. H., Quan, H. N., Ramaswamy, N. T., Zhang, L., Barik, S., Zheng, J., Cannon, J. F., Lee, E. Y., and Shenolikar, S. (1998) *J. Biol. Chem.* **273,** 27716–27724
13. Zheng, J., Khalil, M., and Cannon, J. F. (2000) *J. Biol. Chem.* **275,** 18070–18078
14. Wek, R. C., Cannon, J. F., Dever, T. E., and Hinnebusch, A. G. (1992) *Mol. Cell. Biol.* **12,** 5700–5710
15. Dever, T. E. (1998) *Methods Mol. Biol.* **77,** 167–178
16. Connor, J. H., Quan, H., Oliver, C., and Shenolikar, S. (1998) *Methods Mol. Biol.* **93,** 41–58
17. Ceulemans, H., and Bollen, M. (2004) *Physiol. Rev.* **84,** 1–39
18. Oliver, C. J., and Shenolikar, S. (1998) *Front. Biosci.* **3,** D961–D972
19. Nimmo, G. A., and Cohen, P. (1978) *Eur. J. Biochem.* **87,** 341–351
20. Allen, P. B., Hvalby, O., Jensen, V., Errington, M. L., Ramsay, M., Chaudhry, F. A., Bliss, T. V., Storm-Mathisen, J., Morris, R. G., Andersen, P., and Greengard, P. (2000) *J. Neurosci.* **20,** 3537–3543
21. Scrimgeour, A. G., Allen, P. B., Fienberg, A. A., Greengard, P., and Lawrence, J. C., Jr. (1999) *J. Biol. Chem.* **274,** 20949–20952
22. Aleem, E. A., Flohr, T., Hunziker, A., Mayer, D., Bannasch, P., and Thielmann, H. W. (2001) *Mol. Cell. Biochem.* **217,** 1–12
23. Brush, M. H., Weiser, D. C., and Shenolikar, S. (2003) *Mol. Cell. Biol.* **23,** 1292–1303
24. Jousse, C., Oyadomari, S., Novoa, I., Lu, P., Zhang, Y., Harding, H. P., and Ron, D. (2003) *J. Cell Biol.* **163,** 767–775
25. Terry-Lorenzo, R. T., Elliot, E., Weiser, D. C., Prickett, T. D., Brautigan, D. L., and Shenolikar, S. (2002) *J. Biol. Chem.* **277,** 46535–46543
26. Eto, M., Karginov, A., and Brautigan, D. L. (1999) *Biochemistry* **38,** 16952–16957
27. Koyama, M., Ito, M., Feng, J., Seko, T., Shiraki, K., Takase, K., Hartshorne, D. J., and Nakano, T. (2000) *FEBS Lett.* **475,** 197–200
28. Kwon, Y. G., Huang, H. B., Desdouits, F., Girault, J. A., Greengard, P., and Nairn, A. C. (1997) *Proc. Natl. Acad. Sci. U. S. A.* **94,** 3536–3541
29. Bibb, J. A., Snyder, G. L., Nishi, A., Yan, Z., Meijer, L., Fienberg, A. A., Tsai, L. H., Kwon, Y. T., Girault, J. A., Czernik, A. J., Huganir, R. L., Hemmings, H. C., Jr., Nairn, A. C., and Greengard, P. (1999) *Nature* **402,** 669–671
30. Eto, M., Elliott, E., Prickett, T. D., and Brautigan, D. L. (2002) *J. Biol. Chem.* **277,** 44013–44020
31. MacDougall, L. K., Campbell, D. G., Hubbard, M. J., and Cohen, P. (1989) *Biochim. Biophys. Acta* **1010,** 218–226
32. Sakagami, H., Ebina, K., and Kondo, H. (1994) *Brain Res: Mol. Brain Res.* **25,** 7–18
33. Hemmings, H. C., Jr., Girault, J. A., Nairn, A. C., Bertuzzi, G., and Greengard, P. (1992) *J. Neurochem.* **59,** 1053–1061
34. McLaren, L., Boyle, S., Mason, J. O., and Bard, J. B. (2000) *Mech. Dev.* **96,** 237–241
35. Alberts, A. S., Montminy, M., Shenolikar, S., and Feramisco, J. R. (1994) *Mol. Cell. Biol.* **14,** 4398–4407
36. Chyan, C. L., Tang, T. C., Chen, Y., Liu, H., Lin, F. M., Liu, C. K., Hsieh, M. J., Shiao, M. S., Huang, H., and Lin, T. H. (2001) *J. Biomol. NMR* **21,** 287–288
37. Levin, D., Ernst, V., and London, I. M. (1979) *J. Biol. Chem.* **254,** 7935–7941
38. Foulkes, J. G., Cohen, P., Strada, S. J., Everson, W. V., and Jefferson, L. S. (1982) *J. Biol. Chem.* **257,** 12493–12496
39. Towle, C. A., Mankin, H. J., Avruch, J., and Treadwell, B. V. (1984) *Biochem. Biophys. Res. Commun.* **121,** 134–140
40. Preedy, V. R., and Garlick, P. J. (1988) *Biochem. J.* **251,** 727–732
41. Kimball, S. R., and Jefferson, L. S. (1994) *Biochimie (Paris)* **76,** 729–736

THE JOURNAL OF BIOLOGICAL CHEMISTRY
Vol. 280, No. 16, Issue of April 22, pp. 15903–15911, 2005
Printed in U.S.A.

Importance of a Surface Hydrophobic Pocket on Protein Phosphatase-1 Catalytic Subunit in Recognizing Cellular Regulators*

Received for publication, January 24, 2005
Published, JBC Papers in Press, February 9, 2005, DOI 10.1074/jbc.M500871200

Jennifer A. Gibbons‡, Douglas C. Weiser, and Shirish Shenolikar§

From the Department of Pharmacology and Cancer Biology, Duke University Medical Center, Durham, North Carolina 27710

Cellular functions of protein phosphatase-1 (PP1), a major eukaryotic serine/threonine phosphatase, are defined by the association of PP1 catalytic subunits with endogenous protein inhibitors and regulatory subunits. Many PP1 regulators share a consensus RVXF motif, which docks within a hydrophobic pocket on the surface of the PP1 catalytic subunit. Although these regulatory proteins also possess additional PP1-binding sites, mutations of the RVXF sequence established a key role of this PP1-binding sequence in the function of PP1 regulators. WT PP1α, the C-terminal truncated PP1α-(1–306), a chimeric PP1α containing C-terminal sequences from PP2A, another phosphatase, PP1α-(1–306) with the RVXF-binding pocket substitutions L289R, M290K, and C291R, and PP2A were analyzed for their regulation by several mammalian proteins. These studies established that modifications of the RVXF-binding pocket had modest effects on the catalytic activity of PP1, as judged by recognition of substrates and sensitivity to toxins. However, the selected modifications impaired the sensitivity of PP1 to the inhibitor proteins, inhibitor-1 and inhibitor-2. In addition, they impaired the ability of PP1 to bind neurabin-I, the neuronal regulatory subunit, and G_M, the skeletal muscle glycogen-targeting subunit. These data suggested that differences in RVXF interactions with the hydrophobic pocket dictate the affinity of PP1 for cellular regulators. Substitution of a distinct RVXF sequence in inhibitor-1 that enhanced its binding and potency as a PP1 inhibitor emphasized the importance of the RVXF sequence in defining the function of this and other PP1 regulators. Our studies suggest that the diversity of RVXF sequences provides for dynamic physiological regulation of PP1 functions in eukaryotic cells.

Early studies by Ingebritsen and Cohen (1, 2) classified mammalian protein serine/threonine phosphatases into two major groups, type-1 and type-2, based in large part on their sensitivity to two endogenous protein inhibitors, inhibitor-1 (I-1)[1] and inhibitor-2 (I-2). Type-I protein serine/threonine phosphatase or protein phosphatase-1 (PP1), displays unique and potent inhibition by nanomolar concentrations of I-1 and I-2. In contrast, PP2A and other type-2 protein phosphatases are essentially resistant to these inhibitor proteins. To date, more than 50 PP1-interacting proteins have been identified (3). Some, like I-1 and I-2, function as PP1 inhibitors, whereas others represent targeting subunits that direct subcellular localization and substrate recognition by multiprotein complexes containing PP1 catalytic subunits. Remarkably, PP1 and PP2A catalytic subunits share nearly 50% primary sequence identity, which may account for their overlapping substrate specificity *in vitro* (1). However, all PP1 regulators thus far analyzed demonstrate the unique ability displayed by I-1 and I-2 to selectively associate with PP1 and modify its catalytic function.

Detailed structure-function analyses of I-1 (4) and its neuronal homologue, DARPP-32 (5), first highlighted the tetrapeptide sequence KIQF, which acts in conjunction with PKA phosphorylation at a conserved threonine to inhibit PP1 activity. Subsequent studies noted a homologous sequence, RVSF, in the skeletal muscle glycogen targeting subunit, G_M, that was also required for PP1 binding (6). Cocrystallization of PP1 with a synthetic dodecapeptide encompassing the RVSF sequence from G_M established the RVXF motif as a conserved PP1-binding sequence that associates with a hydrophobic pocket on the surface of the PP1 catalytic subunit (7).

There are extensive surface interactions between PP1 and regulatory subunits, as demonstrated by alanine-scanning mutagenesis of yeast PP1 (8) and the recently resolved structure of PP1 catalytic subunit complexed with the myosin-targeting subunit, MYPT1 (9). However, the ability of RVXF-containing peptides derived from several PP1 regulatory subunits to displace G_M from the glycogen-bound PP1 complex suggested a critical role for the RVXF sequence in PP1 binding (7). Single amino acid substitutions (*e.g.* Phe to Ala) in the RVXF motif severely impaired or abolished the ability of PP1 regulatory subunits (10) and inhibitors (4) to bind and regulate PP1. This emphasized the pivotal role played by the RVXF motif in PP1 binding and regulation. Several studies have identified RVXF-containing PP1-binding proteins using an overlay or far-Western with an isolated PP1 catalytic subunit (11, 12). Although this technique successfully identified many regulators, the pro-

* This work was supported in part by National Institutes of Health (NIH) Grant DK52054 (to S. S.). The costs of publication of this article were defrayed in part by the payment of page charges. This article must therefore be hereby marked "*advertisement*" in accordance with 18 U.S.C. Section 1734 solely to indicate this fact.

‡ Supported by NIH Toxicology Predoctoral Training Award T32-ES-07031.

§ To whom correspondence should be addressed: Cardiovascular Molecular Sciences, Pfizer Global Research and Development, 2800 Plymouth Road, Ann Arbor, MI 48105. Tel: 734-622-8211; Fax: 734-622-1355; E-mail: shirish.shenolikar@Pfizer.com.

[1] The abbreviations used are: I-1, inhibitor-1; I-2, inhibitor-2; PP1, protein phosphatase-1; PP2A, protein phosphatase-2A; WT, wild-type; MYPT1, myosin phosphatase targeting subunit; DARPP-32, dopamine and cAMP-regulated phosphoprotein; CHRM2, a chimera of $PP1^{1-273}$ and $PP2A^{267-309}$; G_M, skeletal muscle glycogen-targeting subunit; MCLR, microcystin-LR; MBP, myelin basic protein; GST, glutathione *S*-transferase; Nrb, neurabin-I; GADD34, growth arrest and DNA-damage-inducible protein; PKA, protein kinase A; ATPγS, adenosine 5′-*O*-(thiotriphosphate); TBS, Tris-buffered saline.

totypic PP1 regulators I-1 and I-2 were either weakly or not detected using this technique. This suggested that not all RVXF sequences were equivalent in PP1 binding. Direct binding studies also indicated that the unphosphorylated forms of I-1 (4) and DARPP-32 (5) bind PP1 very weakly. Although PKA phosphorylation activates these proteins as nanomolar inhibitors of PP1, the covalent modification only modestly increased their affinity for the PP1 catalytic subunit. Comparison of RVXF-containing synthetic peptides modeled on I-1 and G_M in their ability to disrupt neuronal PP1 complexes (13) also highlighted their differing affinities for PP1. Substituting the PP1-binding motif from nuclear inhibitor of PP1, RVTF, in place of the KIQF sequence normally found in I-1 enhanced its potency as a PP1 inhibitor, and emphasized the key role played by the RVXF sequence in defining the function of PP1 regulators (12). These studies suggested that the differences in the association of this conserved sequence with the common binding site on the PP1 catalytic subunit defined its physiological regulation of cellular PP1 regulators.

Our earlier studies (14) that substituted C-terminal sequences from PP2A in PP1α highlighted the diminished ability of the chimeric phosphatase, CHRM2, to bind I-1, I-2, nuclear inhibitor of PP1, and G_M. Later studies (15) showed similar deficits in CHRM2 binding to two other PP1 regulators, PP1 nuclear targeting subunit and spinophilin. Together, these studies suggested that the C-terminal sequences unique to PP1α played a key role in PP1 binding and regulation by cellular proteins. Attempts to reverse these regulatory defects in CHRM2 by systematic substitution of PP1-specific sequences in the PP2A-derived C terminus highlighted a PP1-specific sequence, ^{290}MC^{291}, that enhanced the potency of DARPP-32 as an inhibitor of the modified CHRM2 (15). These and other data suggested that Met^{290} and Cys^{291}, which line the hydrophobic RVXF-binding pocket and interact with the RVXF sequences in G_M (7) and MYPT1 (9), played a key role in PP1 regulation by cellular regulators. However, substitution of ^{290}MC^{291} in CHRM2 had little effect on its decreased inhibition by I-2. This suggested that the hydrophobic pocket on the PP1 catalytic subunit could distinguish RVXF motifs present in different regulators and thereby differentiate the ability of these proteins to regulate PP1 activity.

Current studies deleted or substituted C-terminal sequences in PP1α as well as specifically modifying selected amino acids in the hydrophobic pocket of PP1α to define the role of the surface hydrophobic pocket in the recognition of RVXF-containing proteins. Our studies provided the first direct experimental evidence that the affinity of cellular regulators for the PP1 catalytic subunit is dictated by the RVXF sequence present in these proteins, and that the docking of this RVXF sequence in the surface hydrophobic pocket is conserved in all PP1 isoforms. Implications of these findings for the physiological regulation of PP1 in eukaryotic cells will be discussed.

EXPERIMENTAL PROCEDURES

Materials—Phosphorylase *b* was purchased from Calzyme, and phosphorylase kinase was obtained from Invitrogen. Anti-PP1 monoclonal antibody was obtained from Santa Cruz Biotechnology, and horseradish peroxidase-conjugated anti-digoxigenin antibody was from US Biological. [γ-^{32}P]ATP (3000 Ci/mmol) was purchased from Amersham Biosciences. Heparin-agarose was purchased from Bio-Rad. Digoxigenin-NHS (*N*-hydroxysuccinimide) was obtained from Roche Applied Science. *N*-Hydroxysuccinimide-activated Sepharose (Amersham Biosciences) was used to make microcystin-LR-Sepharose (MCLR-Sepharose) (16), and glutathione-Sepharose was obtained from Amersham Biosciences. MCLR and okadaic acid were purchased from Alexis Corp. Bacterial expression vector, pKK223-3, containing a cDNA encoding human PP1α-(1–306) (PP1306) with additional seven C-terminal residues derived from the plasmid sequences, and the PP1α/PP2ACα chimeric catalytic subunit, CHRM2 (17), were provided by Richard Honkanen (University of South Alabama). The expression plasmid pTACTAC for full-length human PP1α (18) was obtained from Ernest Y.C. Lee (New York Medical College). Purified PP2A catalytic subunit (19) was provided by Brian Wadzinski (Vanderbilt University). The plasmid pGEX-2T containing the cDNA-encoding GST-I-1 was previously described (4), and GST-I-1_{RVTF} (12) was from Mathieu Bollen (Katholieke Universiteit, Leuven). The pET8d-inhibitor-2 plasmid (20) was from Anna DePaoli-Roach (Indiana University). The expression plasmid encoding GST-G_M-(1–240) (10) was provided by David L. Brautigan (University of Virginia), and GST-neurabin I-(374–516) was previously described (21).

Mutation of the PP1306 Catalytic Subunit—Point mutations L289R, M290K, and C291R were created in human PP1306 using the QuikChange site-directed mutagenesis kit (Stratagene). For L289R, the following primers, 5′-GAGTGTGGACGAGACCAGAATGTGCTCTTTCCAGATCCTC and 5′-GAGGATCTGGAAAGAGCACATTCTGGTCTCGTCCACACTC, for M290K, 5′-GTGGACGAGACCCTCAAGTGCTCTTTCCAGATCC and 5′-GGATCTGGAAAGAGCACTTGAGGGTCTCGTCCAC and for C291R, 5′-GTGGACGAGACCCTCATGAGATCTTTCCAGATCC and 5′-GGATCTGGAAAGATCTCATGAGGGTCTCGTCCAC were utilized. All mutations were verified by sequence analysis.

Purification of Recombinant PP1α Catalytic Subunits—All PP1α catalytic subunits were expressed in *Escherichia coli* BL21 grown overnight in Luria Broth containing 1 mM $MnCl_2$ and 50 μg/ml ampicillin (Sigma). Protein expression was induced by addition of 50 μM isopropyl-β-D-thiogalactopyranoside (Gold Technologies), with continued growth of the bacteria at 18 °C until A_{600} of culture was 0.6–0.8. Bacteria were sedimented at 4,000 × *g* for 10 min and resuspended in 50 mM Tris-HCl, pH 7.5, containing 0.1% (v/v) 2-mercaptoethanol, 1 mM EDTA, 1 mM $MnCl_2$, and 10% (v/v) glycerol (Buffer A) containing the protease inhibitors 1 mM phenylmethylsulfonyl fluoride, 1 mM benzamidine, 1 μg/ml aprotinin, 1 μg/ml leupeptin, 1 μg/ml pepstatin A. Bacteria were lysed using French press (~19,000 p.s.i.), and cell debris was removed by centrifugation at 30,000 × *g* for 30 min. The cleared lysates were subjected to chromatography on either heparin-agarose or MCLR-Sepharose to isolate PP1 catalytic subunits.

For purification on heparin-agarose, bacterial extract was applied to the matrix in Buffer A and washed extensively with Buffer A containing 0.1 M NaCl. PP1 catalytic subunits were eluted with Buffer A containing 0.5 M NaCl. Fractions were collected and assayed for PP1 activity. Fractions were pooled, dialyzed overnight against Buffer A, concentrated using Centricon-10 (Pall Life Sciences), and dialyzed extensively against Buffer A containing 55% (v/v) glycerol prior to storage at −20 °C. Purification of PP1 catalytic subunits on MCLR-Sepharose was undertaken essentially as described by Moorhead *et al.* (16), and stored as described above.

Preparation of Recombinant PP1 Regulators—GST-I-1 fusion proteins were expressed, and phosphorylated as described (22), with the following modifications: bacteria were lysed by two passages through French press at ~19,000 p.s.i. The fusion proteins were purified via glutathione-Sepharose according to manufacturer's instructions (Amersham Biosciences). GST-neurabin-I-(374–516) and GST-G_M-(1–240) were expressed and purified as described (21). I-1 (23) and I-2 (12) were expressed and purified as previously described.

^{32}P-Phosphoprotein Substrates—For phosphorylase *a*, phosphorylase kinase (0.25 mg) was added to a solution of phosphorylase *b* (10 mg/ml) in 100 mM β-glycerol phosphate and 100 mM Tris-HCl, pH 8.2, containing 1 mM $MgCl_2$, 100 μM ATP, 0.2 mM $CaCl_2$, 0.1% (v/v) 2-mercaptoethanol, and 250–300 μCi of [γ-^{32}P]ATP, and incubated at 37 °C. At 30-min intervals, aliquots (10 μl) of the reaction mixture were removed and added to 200 μl of 20% (v/v) trichloroacetic acid and 50 μl of bovine serum albumin (10 mg/ml). The sample was placed on ice for 2 min, then centrifuged at 15,000 × *g* for 10 min. The pellet was repeatedly washed with 20% (w/v) trichloroacetic acid prior to Cerenkov counting. Once the ^{32}P incorporation reached a plateau (~90 min), the reaction was stopped by the addition of an equal volume of 90% saturated ammonium sulfate and placed on ice for 20 min. The mixture was centrifuged at 20,000 × *g* for 20 min, and the sedimented protein was washed twice with ice-cold 45% saturated ammonium sulfate. The pellet was then resuspended in 50 mM Tris-HCl, pH 7.5, 1 mM EDTA, and 0.1% (v/v) 2-mercaptoethanol, and dialyzed extensively against the same buffer.

For myelin basic protein (MBP), 200 μg of MBP was added to a solution of 1 mM ATP, 10 mM $MgCl_2$, 10–20 μCi of [γ-^{32}P]ATP, and 50 mM Tris-HCl, pH 7.5. Then, 10–20 μl of purified PKA was added to the reaction and incubated at 37 °C. ^{32}P incorporation was examined in the same manner as phosphorylase *a*, and as the ^{32}P incorporation reached a plateau, the reaction was placed in dialysis buffer (50 mM Tris-HCl,

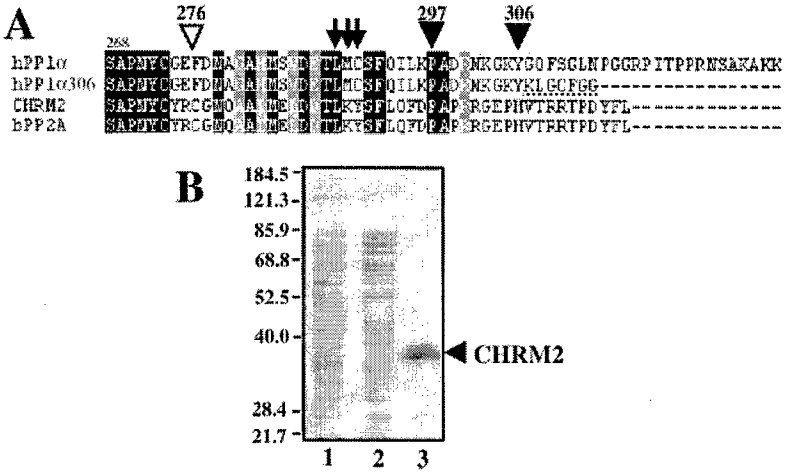

FIG. 1. **Isolation of recombinant human PP1α catalytic subunits.** *A*, the C-terminal sequences of WT human PP1α, PP1306, CHRM2, and bovine PP2A are shown via ClustalW alignment (50). Amino acid identities are shown as *white letters* against a *black background*, and homologous residues are against a *gray background*. The *arrows* point at three residues in PP1306, Leu[289], Met[290], and Cys[291] that were mutated and analyzed in this study. The *closed arrowheads* indicate C-terminal deletions of PP1α that yielded active phosphatases. PP1α-(1–306) was analyzed in this study, whereas -(1–297) was previously analyzed (31). The C-terminal truncated PP1-(1–276), shown by the *open arrowhead*, was inactive. PP1306 also contained additional residues (*underlined*) derived from the plasmid pKK223–2. *B*, representative purification of a PP1 mutant, CHRM2, is shown using SDS-PAGE. *Lane 1*, crude bacterial extract; *lane 2*, CHRM2 purified on heparin-agarose; and *lane 3*, CHRM2 purified on MCLR-Sepharose.

pH 7.5, 1 mM EDTA, and 0.1% (v/v) 2-mercaptoethanol), with frequent changes until background ^{32}P diminished.

Protein Phosphatase Assays—PP1 catalytic subunits diluted in 50 mM Tris-HCl, pH 7.5, containing 1 mM $MnCl_2$, 0.1% (v/v) 2-mercaptoethanol, and 1 mg/ml bovine serum albumin were incubated with [^{32}P]phosphorylase *a* (2 mg/ml) at 37 °C for 10 min (total reaction volume of 60 μl). Reaction was terminated by addition of 200 μl of 20% (v/v) trichloroacetic acid and 50 μl of bovine serum albumin (10 mg/ml), and the mixture was centrifuged at 15,000 × *g* for 5 min. [^{32}P]Phosphate released into the supernatant was measured by liquid scintillation counting. Assays using MBP as substrate were performed in the same manner, using 10 μM MBP per reaction.

To assay PP1 inhibition by I-1, recombinant I-1 was first incubated with 0.3 mg/ml PKA, 50 mM Tris-HCl, pH 7.5, 0.2 mM ATPγS, and 2 mM $MgCl_2$ at 30 °C for 72 h. The thiophosphorylated I-1 was dialyzed into 50 mM Tris-HCl, pH 7.5, 0.005% (v/v) Brij-35, and 0.1% 2-mercaptoethanol. Thiophosphorylated I-1 was briefly incubated with PP1 before the addition of phosphorylase *a*. In assays for PP1 inhibition by I-2, the I-2 protein was preincubated with PP1 for 20 min at 37 °C, and targeting subunits were preincubated with PP1 for 5 min at 37 °C prior the initiation of the phosphatase assay.

PP1 Sedimentation—GST fusions of PP1 inhibitors and/or targeting subunits were incubated with glutathione-Sepharose (25-μl bed volume) equilibrated in Tris-buffered saline (TBS) (50 mM Tris-HCl, pH 7.5, 150 mM NaCl) for 1 h at 4 °C. The beads were washed twice with TBS, and incubated for 1 h at 4 °C with bovine serum albumin (1 mg/ml). They were then washed twice with TBS, and recombinant PP1 was added for 1 h at 4 °C. The beads were washed four times with NETN-250 (250 mM NaCl, 1 mM EDTA, 10 mM Tris-HCl, pH 7.5, and 0.5% (v/v) Nonidet P-40). Bound proteins were eluted with SDS sample buffer, and subjected to SDS-PAGE on 12% (w/v) polyacrylamide gels. Proteins were electrophoretically transferred to polyvinylidene difluoride membranes, which were stained with Ponceau S to visualize the proteins. Membranes were blocked in 4% milk (w/v) in TBS plus 0.05% Tween, and PP1 detected by immunoblotting with an anti-PP1 antibody. The protein bands were quantified by scanning using Quantity One software (Bio-Rad).

PP1 Far-Western Blots—PP1 overlays were performed as described (11), with the following modifications. Protein staining using Ponceau S verified equivalent protein loading. The bound digoxigenin-labeled PP1 was detected by immunoblotting with an anti-digoxigenin antibody (horseradish peroxidase-linked) and ECL reaction (PerkinElmer Life Sciences). To ensure linearity of the overlay assays in each case, the ECL reaction was exposed to film for 2, 15, and 30 s.

For these assays, GST-I-1 was phosphorylated using PKA (0.2 μg/ml), 100 μM ATP, 1 mM $MgCl_2$, at 37 °C for 90 min. Phospho-GST-I-1 was dialyzed into 50 mM Tris-HCl, pH 7.5, 0.005% (v/v) Brij-35, and 0.1% (v/v) 2-mercaptoethanol. GST was similarly phosphorylated using PKA for control pull-down assays. PP1 binding to GST alone was defined as nonspecific and subtracted from that bound to GST fusion proteins containing known PP1 regulators. Protein concentration was determined using the Bio-Rad protein assay with BSA (Pierce) as the standard.

Analysis of PP1 Structure—The program Rasmol 2.6 (24) was used to generate the PP1 structure, as well as the programs Mage and Prekin (25), and interaction dots were generated with Molprobity (26) and Probe (27). The latter four programs were obtained from kinemage.biochem.duke.edu.

RESULTS

Purification of Recombinant PP1 Catalytic Subunits—Emerging studies (21, 28, 29) showed that PP1 regulators displayed selectivity for distinct PP1 isoforms, which differed largely in their C-terminal sequences. Prior studies (30, 31) suggested that extensive deletions of C-terminal sequences impaired or destabilized PP1α activity. Although recombinant PP1α-(1–297) demonstrated phosphorylase phosphatase activity equivalent to that of full-length PP1α, PP1α-(1–276) was not expressed in bacteria. To focus on the role of the RVXF-binding site conserved in all PP1 isoforms, we expressed PP1α-(1–306) (PP1306), which eliminated the majority of C-terminal residues unique to this PP1 isoform. We also analyzed PP1α and CHRM2, which contains PP1α-(1–273) fused to the C-terminal 43 amino acids from bovine PP2Aα catalytic subunit, previously shown to generate an active phosphorylase phosphatase that was resistant to many PP1 regulators (14). In addition, we expressed PP1306 with the single amino acid substitutions L289R, M290K, and C291R to modify the RVXF-binding pocket, which introduced residues more commonly found in type-2 phosphatases.

Previous studies utilized heparin-agarose to separate PP1 from type-2 protein serine/threonine phosphatases (32) and purify recombinant PP1 catalytic subunit expressed in *E. coli* (18). Complete purification of PP1, however, required multiple chromatographic steps and reduced the yields of this protein (18). Comparison of a recombinant PP1 catalytic subunit, such as CHRM2 (Fig. 1*B*), purified from bacterial extracts using either heparin-agarose or affinity chromatography with MCLR immobilized on Sepharose (16), demonstrated that MCLR-Sepharose yielded an essentially single polypeptide (>95% purity) as judged by SDS-PAGE (Fig. 1*B*, *lane 3*). By comparison, chromatography on heparin-agarose (Fig. 1*B*, *lane 2*), although eliminating >90% of bacterial proteins, yielded a preparation of CHRM2 that still contained other proteins. MCLR (IC_{50} < 1

TABLE I

Biochemical properties of WT and mutant PP1α catalytic subunits

All PP1 catalytic subunits were expressed in *E. coli* and purified using affinity chromatography on MCLR-Sepharose. All assays were carried out in duplicate and undertaken at least 3 times, except those in footnote *a*, which were only carried out once in duplicate. The values obtained are shown with standard errors.

	IC_{50}				Phosphorylase *a*	MBP
	Okadaic acid	I-1	I-2	Nrb		
	nM				%	
PP1α	157 ± 11	25[a]	2 ± 0.1	1.75 ± 0.1	39 ± 1	28 ± 0.5
PP1306	133 ± 23	29 ± 5	4.3 ± 0.5	7.3 ± 0.6	100	100
L289R	84 ± 31	66 ± 13	19 ± 6	380 ± 120	72 ± 4	40 ± 3
M290K	69 ± 21	52 ± 2	11 ± 0.5	115 ± 15	117 ± 5	76 ± 3
C291R	97 ± 29	285 ± 5	54 ± 11	>1 μM	71 ± 6	28 ± 1
CHRM2	18 ± 1	380[a]	1,375 ± 675	>1 μM	158 ± 7	103[a]

[a] Assay was carried out once in duplicate.

nM) bound PP1 tightly, requiring strong chaotropic agents (*e.g.* 3 M NaSCN) to elute the phosphatase. However, following dialysis, PP1 preparations purified by either MCLR-Sepharose or heparin-agarose displayed similar phosphorylase phosphatase activity; their specific activities reflected the relative content of the 37-kDa polypeptide representing PP1 catalytic subunit identified by anti-PP1 immunoblots (data not shown). This was consistent with previous findings of Campos *et al.* (33), which demonstrated that chromatography on MCLR-Sepharose provided preparations of purified recombinant PP1 catalytic subunits with excellent specific activity.

Using MCLR-Sepharose, we purified recombinant PP1α and several PP1 mutants to near homogeneity. We first assessed the relative enzymatic activity of the purified phosphatases using two different substrates, phosphorylase *a* and MBP (Table I). Compared with PP1306, PP1α showed slightly reduced activity against both substrates. In contrast, CHRM2 showed either similar or slightly increased activity. These findings may be consistent with earlier observations (34) that the extreme C-terminal sequences specific to PP1α partially inhibited or suppressed its enzymatic activity. Thus, the deletion of amino acids 306–330 in PP1306 or substitution of PP2A C-terminal sequences in CHRM2 may increase the intrinsic activity of these PP1 catalytic subunits. Further introduction of the point mutations L289R, M290K, or C291R resulted in a slight reduction of activity when compared with PP1306, but the activity of these mutant catalytic subunits was either equal to or higher than that of PP1α against both phosphoprotein substrates.

Toxin Sensitivity of WT and Mutant PP1α Catalytic Subunits—Most xenobiotic inhibitors bound at the catalytic site of the PP1 catalytic subunit (35–37). Thus, sensitivity of mutant PP1α subunits to one or more toxins provided evidence of structural alterations at or near the catalytic site. Compared with PP1α (MCLR IC_{50} = 1.1 ± 0.2 nM), deletion of PP1α-specific C-terminal sequences in PP1306 (MCLR IC_{50} = 0.7 ± 0.1 nM) had no discernable effect on its sensitivity to either MCLR or okadaic acid. By comparison, CHRM2, which showed a similar IC_{50} for MCLR (38), was much more sensitive to okadaic acid than PP1α or PP1306 (Table I and Fig. 2*A*). MCLR is an equipotent inhibitor of PP1 and PP2A. In contrast, okadaic acid demonstrates an IC_{50} for PP2A, which is ~100-fold lower than that for PP1 (38). These data confirmed that the β12-β13 loop played a key role in defining the sensitivity of PP1 to okadaic acid (14). Thus, PP1306, which retains the β12-β13 loop of PP1α, was inhibited by okadaic acid in a manner indistinguishable from PP1α (Fig. 2*A*). By comparison, CHRM2, which incorporates the β12-β13 loop of PP2A, displayed nearly 10-fold greater sensitivity to okadaic acid compared with either PP1α or PP1306. Further introduction of L289R, M290K, or C291R in PP1306 had only a modest impact on the sensitivity of PP1 catalytic subunits to okadaic acid. Essentially identical results were obtained with

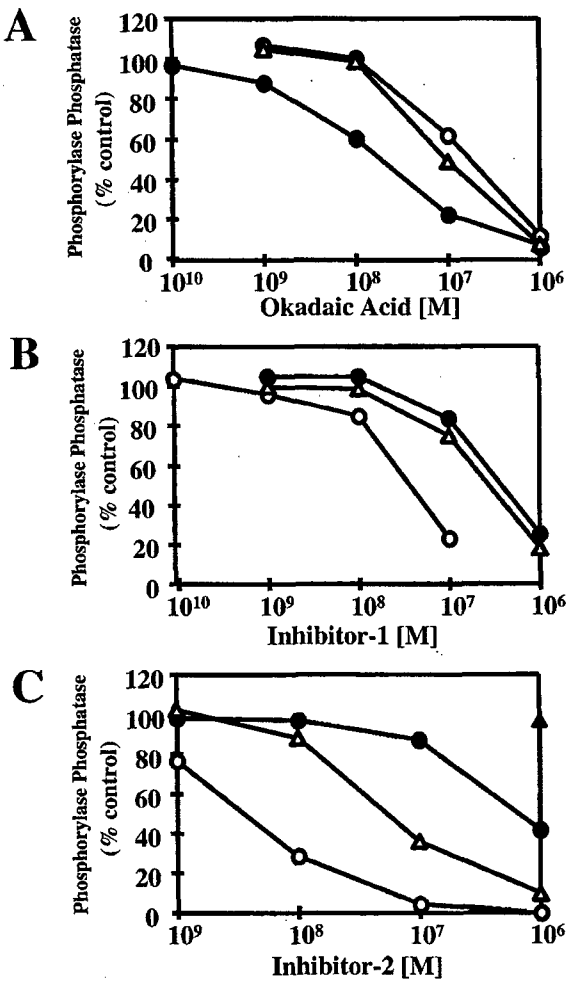

FIG. 2. **The C-terminal substitution, C291R, renders PP1306 resistant to protein inhibitors.** Inhibition of phosphorylase phosphatase activity by okadaic acid (*A*), inhibitor-1 (*B*), and inhibitor-2 (*C*) was analyzed as described under "Experimental Procedures." Representative curves demonstrating the dose-dependent inhibition of PP1306 (*open circles*), CHRM2 (*closed circles*), and PP1306 C291R (*open triangles*) are shown.

PP1 catalytic subunits purified on heparin-agarose (data not shown), demonstrating that the potentially harsh conditions used to elute PP1 from MCLR-Sepharose did not modify the catalytic sites of these phosphatases.

Inhibition of WT and Mutant PP1α Catalytic Subunits by Inhibitor Proteins—PP1 is characterized by its unique sensitivity to the mammalian proteins I-1 and I-2. Although nanomolar concentrations of I-2 or PKA-phosphorylated I-1 inhibit PP1 activity (38), high micromolar concentrations of these pro-

teins have no effect on PP2A activity (4). In this regard, sensitivity of PP1306 to I-1 and I-2 was essentially identical to that of PP1α, indicating that the deletion of the C-terminal 24 amino acids had no effect on PP1 recognition by these protein regulators. However, as noted in previous studies (14), CHRM2 with the PP2A C terminus showed more than a 10-fold reduction in its IC_{50} for I-1 and a nearly 500-fold reduced IC_{50} for I-2 compared with either PP1α or PP1306 (Table I). This defect could result from the altered β12-β13 loop, previously shown to dictate sensitivity from PP1 to I-1 and I-2, or the absence of critical amino acids constituting the surface hydrophobic pocket that binds RVXF motifs present in I-1 (14, 23) and I-2 (39).

Although some modifications of the RVXF-binding pocket, L289R and M290K, showed modest decrements in IC_{50} values for I-1 and I-2, C291R showed a dramatic loss in its sensitivity for I-1. The nearly 10-fold decrease in IC_{50} for I-1 was almost equal to that seen with CHRM2 (Table I and Fig. 2*B*). This suggested that the substitution of a single amino acid, C291R, in PP1306 attenuated PP1 regulation by I-1 to the same extent as removal of 53 amino acids from the PP1α C terminus and their replacement by 42 amino acids of the PP2A C terminus, which generated CHRM2. This highlighted the critical importance of the surface hydrophobic pocket for PP1 regulation by I-1.

All three mutants also showed modest reductions in their sensitivity to I-2. In contrast to M290K and L289R, which showed a reduction of ~3- and 5-fold IC_{50} for I-2, C291R demonstrated a >10-fold decrease in IC_{50} for I-2. On the other hand, the reduction in I-2 sensitivity in all PP1306 mutants was significantly less than that seen in CHRM2 (Table I and Fig. 2*C*). This suggested differences in the mode of action of I-1 and I-2 as PP1 inhibitors. Although the fusion of PP2A C terminus significantly reduced the inhibition of CHRM2 by I-2 (IC_{50} 1.35 μM), the chimeric phosphatase still retained some I-2 binding, consistent with previous studies that suggested that multiple regions of I-2 mediated PP1 binding (39). In contrast, the activity of PP2A was unaffected by 1 μM I-2 (Fig. 2*C*).

Association of WT and Mutant PP1α Catalytic Subunits with Regulatory Subunits—The diversity of RVXF sequences in PP1 regulators (3) and differences in various RVXF-containing peptides to disrupt cellular PP1 complexes (13) suggested that RVXF-containing PP1 regulators differ in their association with the surface hydrophobic pocket on PP1. To investigate PP1 binding to regulatory or targeting subunits with different RVXF sequences, we analyzed a recombinant G_M, which contains the sequence RVSF (10), and a neurabin-I (Nrb) (21) polypeptide with the sequence KIKF; both sequences are required for PP1 binding. Full-length polypeptides, representing G_M (1109 amino acids) and Nrb (1150 amino acids), are either poorly or not expressed in bacteria. Thus, we expressed GST-G_M-(1–240) and GST-Nrb-(374–516), which contain the key elements required for PP1 binding.

The binding of WT and mutant PP1 catalytic subunits to GST-Nrb and GST-G_M was analyzed by sedimentation of these complexes bound to glutathione-Sepharose. The presence of GST fusion proteins was analyzed by protein staining with Ponceau S, and PP1 was detected by immunoblotting with an anti-PP1 antibody. PP1306 binding to GST-Nrb and GST-G_M is shown in Fig. 3*A*. With increasing concentrations of targeting subunit, increased amounts of PP1306 were sedimented. Binding to CHRM2, L289R, M290K, and C291R was analyzed in a similar manner, and the bound PP1 catalytic subunits were quantified by densitometry. Under the conditions of this assay, binding to PP1306 was essentially saturated at 5 and 10 μg of GST-G_M (Fig. 3*B*). PP1α showed greater binding to GST-G_M

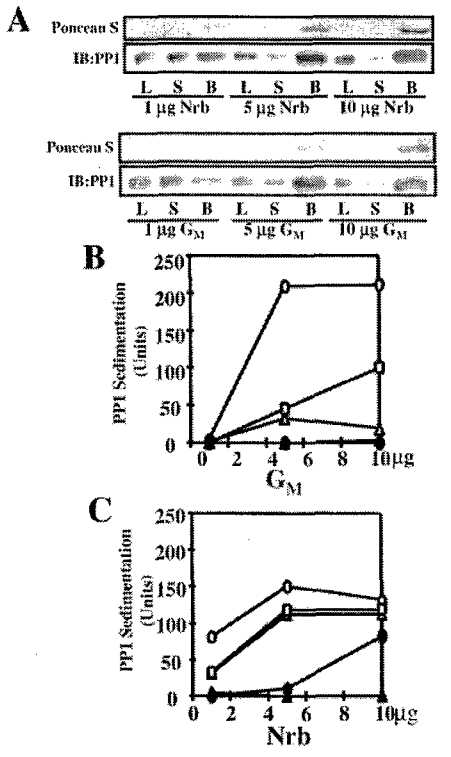

FIG. 3. **The C-terminal substitutions L289R, M290K, and C291R modify PP1306 binding to regulatory subunits.** Sedimentation of WT and mutant PP1306 catalytic subunits was undertaken using the GST-tagged targeting subunits G_M and Nrb. *A* shows a representative PP1306 pull-down, using increasing concentrations of GST-Nrb (*top panel*) and GST-G_M (*bottom panel*). Protein staining using Ponceau S is shown along with anti-PP1 immunoblots. *L*, PP1 load; *S*, supernatant; and *B*, PP1 bound to GST-proteins sedimented using glutathione-Sepharose. *B* compares WT and mutant PP1306 binding to GST-G_M. Dose-dependent binding of PP1306 (*open circles*), L289R (*open triangles*), M290K (*open squares*), C291R (*closed triangles*), and CHRM2 (*closed circles*) is shown. Binding was assessed using densitometry, subtracting nonspecific binding to GST alone, and was expressed in arbitary units. *C* shows the binding of PP1 mutants to GST-Nrb, and was analyzed in a similar manner.

than PP1306, particularly at low concentrations (1 μg) of the GST fusion protein (data not shown). Prior studies (14) suggested that CHRM2 bound more weakly than PP1α to GST-G_M-(1–215). This difference was greatly magnified in our assays, with CHRM2 showing little or no binding to GST-G_M-(1–240). All three point mutants, L289R, M290K, and C291R, were compromised in their ability to bind GST-G_M. Although M290K and L289R bound GST-G_M weakly, C291R, like CHRM2, failed to bind this fusion protein at all concentrations analyzed (Fig. 2*B*). This suggested that, as noted with I-1, the hydrophobic pocket, particularly the amino acid C291, played a critical role in PP1 binding by G_M.

Surprisingly, under conditions that GST-G_M failed to bind CHRM2, GST-Nrb bound CHRM2 weakly, requiring 10 μg of GST-Nrb to visualize significant CHRM2 binding (Fig. 3*B*). This was unexpected as prior studies (15) had demonstrated no binding of CHRM2 to much higher concentrations of GST-spinophilin, a structural homologue of neurabin. This could reflect the use of a different fragment of spinophilin/neurabin-II, namely amino acids 298–817, compared with residues 374–516 of neurabin-I used in this study. Alternately, these differences could be attributed to the different assay conditions or some differences in the primary sequences of the PP1-binding site. Remarkably, unlike GST-G_M, GST-Nrb bound both L289R and M290K almost as effectively as PP1306, indicating that these mutations did not totally disrupt the RVXF-binding

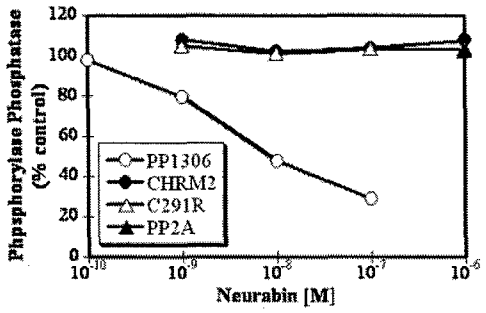

FIG. 4. **The C-terminal substitution C291R renders PP1306 insensitive to inhibition by neurabin-I.** The dose-dependent inhibition of phosphorylase phosphatase activity of PP1306 and mutant phosphatases by GST-Nrb is shown. Representative curves for the inhibition of PP1306 (*open circles*), CHRM2 (*closed circles*), PP1306 C291R (*open triangles*), and PP2A (*closed triangles*) are shown.

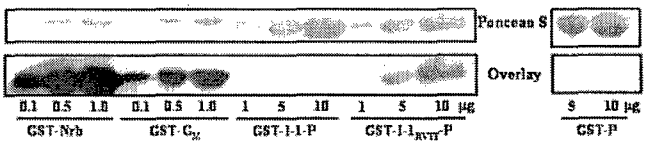

FIG. 5. **PP1306 binding to PP1 regulators.** PP1 overlays using digoxigenin-conjugated PP1 catalytic subunits were undertaken as described under "Experimental Procedures." The *panels* show a representative overlay demonstrating PP1306 binding to increasing concentrations of GST-Nrb, GST-G_M, PKA-phosphorylated GST-I-1, and PKA-phosphorylated GST-I-1_{RVTF}. PKA-phosphorylated GST was used as control. The *upper panel* shows protein staining with Ponceau S, and the *lower panels* shows immunoreactivity to anti-digoxigenin on film exposed for 30 s. Similar experiments were undertaken using other PP1 catalytic subunits and the results are summarized in Table II.

pocket. By comparison, C291R showed little binding to GST-Nrb. These data suggested that Cys^{291} is essential for binding to both GST-G_M and GST-Nrb, but Leu^{289} and Met^{290} play a less critical role in binding of Nrb compared with G_M.

Many PP1 targeting subunits, although promoting PP1 activity against "relevant" substrate(s), inhibited its phosphorylase phosphatase activity. This provides an alternate assay for evaluating the functional effects of PP1 binding by regulators. In contrast to G_M, which only partially inhibits the phosphorylase phosphatase activity of the PP1 catalytic subunit (10), Nrb is a potent PP1 inhibitor in the same assay (21). Thus, GST-Nrb inhibited PP1α with an IC_{50} of ~2 nM (Fig. 4 and Table I). By comparison, PP2A was essentially insensitive to GST-Nrb at concentrations up to 1 μM (Fig. 4). PP1306 was inhibited by GST-Nrb with a modestly reduced $IC_{50} = 7.3 \pm 0.6$ nM. In contrast, neither CHRM2 nor C291R were inhibited by GST-Nrb at up to 1 μM concentration (Fig. 4). L289R and M290K showed ~50-fold and 15-fold reductions in IC_{50} for GST-Nrb, respectively (Table I). Although these experiments emphasized that changes in PP1 binding were not quantitatively linked to the altered enzyme activity, mutations of the RVXF-binding pocket had generally similar effects on both functions. For example, the weakened binding displayed by GST-Nrb for L289R and M290R led to 50- and 15-fold reduction in PP1 inhibitory activity. By contrast, C291R, which failed to bind GST-Nrb in pull-down assays, was unable to inhibit phosphorylase phosphatase activity of PP1 at concentrations up to 1 μM.

Role of the RVXF Sequence in I-1 Function—The above studies suggested that RVXF sequences in various PP1 regulators bound differently within the surface hydrophobic pocket, and thus, were influenced variably by substitutions of different amino acids in the RVXF-binding pocket. To further test this hypothesis, we analyzed WT I-1_{KIQF} and a mutant I-1_{RVTF}. The mutant I-1_{RVTF} was created by substitution of the RVTF sequence derived from nuclear inhibitor of PP1, a PP1-binding protein that can be visualized readily by overlays (12). We utilized an overlay assay in which PP1-binding proteins were subjected to SDS-PAGE, and following electrophoretic transfer to polyvinylidene difluoride membranes, partially renatured. Incubation of membranes with soluble digoxigenin-conjugated PP1 catalytic subunits, followed by immunoblotting with anti-digoxigenin antibody, allowed for direct comparison of PP1 binding to several different target proteins. However, due to the denaturation-renaturation involved in PP1 overlays, this assay favored the detection of PP1 regulators containing RVXF motifs (21).

GST-Nrb and GST-G_M both showed dose-dependent binding by digoxigenin-coupled PP1306 (Fig. 5). By comparison to GST-Nrb and GST-G_M, the PKA-phosphorylated GST-I-1 (GST-I-1-P) bound PP1306 very weakly, requiring 10-fold higher protein for detectable PP1 binding. At similar exposures as Nrb and G_M, PP1306 binding to GST-I-1-P was undetectable. Substitution of the RVTF sequence in GST-I-1 increased PP1306 binding to GST-I-1_{RVTF}-P, albeit the mutant I-1 still bound PP1306 100-fold weaker than GST-G_M. The unphosphorylated GST-I-1 and GST-I-1_{RVTF}, like GST alone, failed to bind any of the PP1 catalytic subunits (data not shown).

The binding of PP1α and mutant PP1 catalytic subunits to several regulators is summarized in Table II. These data showed that, in overlays, PP1306 bound more effectively than PP1α to all regulators analyzed. As noted in pull-down assays, compared with PP1306, all three mutants, L289R, M290K, and C291R, showed reduced binding to GST-G_M. C291R also bound GST-Nrb more weakly than either L289R or M290K. The already weak PP1 binding to GST-I-1-P was essentially abolished by all three mutations in the RVXF-binding pocket. However, substitution of the RVTF sequence in I-1 allowed low but detectable binding by M290K. In general, results obtained with overlays (Table II) paralleled those seen with pull-down assays (Fig. 3). Together, these data suggested that not only the context, namely the parent PP1 regulator, but also the actual RVXF sequence played key roles in defining the affinity of PP1 for cellular regulators.

DISCUSSION

The primary structure of PP1 demonstrates >80% sequence identity from plants to animals, making PP1 one of the most highly conserved proteins in evolution (40). Consistent with its evolutionary conservation, PP1 regulates many critical functions in eukaryotic cells, including transcription, translation, metabolism, cell growth, and differentiation. Regardless of its species origin, PP1 can be readily distinguished from other protein serine/threonine phosphatases by its unique ability to be inhibited by the mammalian inhibitor proteins I-1 and I-2. Both of these PP1 regulators utilize multiple domains to bind and regulate PP1 activity. For example, in addition to the N-terminal KIQF sequence, PKA phosphorylation at threonine-35 is critical for PP1 inhibition by I-1 (4). More recent studies suggested that C-terminal sequences in I-1 also played a role in PP1 binding and regulation (41). Up to five different regions of the I-2 protein are thought to participate in PP1 regulation (39, 42). These and other studies have fostered the hypothesis that cellular regulators have evolved a combinatorial mechanism, utilizing multiple interaction domains, some of which are common to a subset of regulators, to modulate cellular PP1 functions.

Our prior studies utilized a number of different ways to identify the structural determinants on the PP1 catalytic subunit that defined its regulation by cellular proteins. Such studies included the analysis of random mutations (23), surface "charged-to-alanine" substitutions (42), a "core" PP1 catalytic

TABLE II

Comparison of WT and mutant PP1 catalytic subunits binding to mammalian PP1 regulators

PP1 binding was analyzed using overlays as described under "Experimental Procedures," and binding was assessed by chemiluminescence. In three independent experiments, PP1 binding as seen by chemiluminescence was analyzed by exposure of the overlays to film for 2, 15, and 30 s.

	GST-Nrb	GST-G_M	GST-I-1-P	GST-I-1_{RVTF}-P	GST-P
PP1α	++[a]	++	−	+/−	−
PP1306	+++	+++	+/−	+	−
L289R	++	+/−	−	−	−
M290K	++	+/−	−	+/−	−
C291R	+/−	+/−	−	−	−
CHRM2	+/−	+/−	−	−	−

[a] ++ denotes a dark band seen in 15 s; +++ denotes a dark band seen within 2 s; + indicates a dark band in 30 s; +/− denotes a faint band seen in 30 s; and − denotes no bands seen after prolonged exposure.

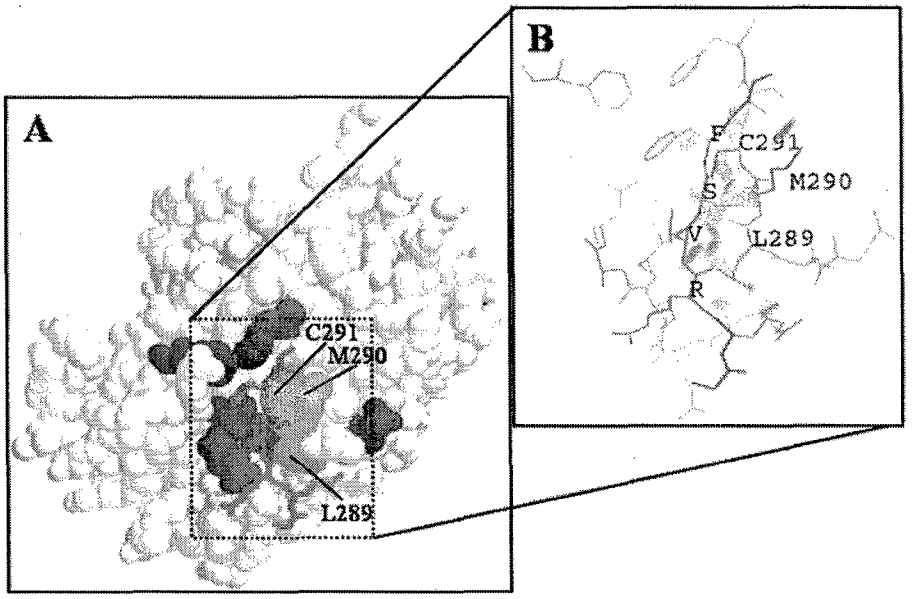

FIG. 6. **Association of the RVXF sequence with the hydrophobic pocket on the PP1 catalytic subunit.** The structure of PP1γ1 bound to a synthetic peptide (representing amino acids 63–75) encompassing the RVSF sequence from the skeletal muscle glycogen-targeting subunit G_M is shown (7). *A*, PP1 is shown in space-fill model using Rasmol. The G_M peptide is shown as a *stick model* in *red*. The amino acids that comprise the RVXF-binding pocket are shown in *blue*, with residues modified in this study (*L289*, *M290*, and *C291*) shown in *cyan*. *B* shows the interactions of Leu^{289} (*red*), Met*290* (*green*), and Cys^{291} (*purple*) with the G_M peptide using the Mage program. The G_M peptide is shown in *red*, and the amino acids lining the RVXF-binding pocket are shown in *gray* with *cyan* side chains. The strength of interactions of the RVSF sequence is displayed as *dots* generated using the Probe program and illustrate associations with Leu^{289} (*red*), Met^{290} (*green*), and Cys^{291} (*purple*).

subunit (amino acids 41–269) that lacked the N- and C-terminal sequences unique to specific PP1 isoforms and a chimeric PP1α (CHRM2), in which the C-terminal PP1 sequences were substituted with those from PP2A (14). Together, these studies highlighted the β12-β13 loop (amino acids 269–282) overhanging the catalytic site as a key determinant defining the sensitivity of PP1 to selected toxins and endogenous PP1 inhibitors, specifically I-1 and I-2. Comparative studies of PP1α and CHRM2 also suggested that the C terminus played a role in the affinity of PP1 for targeting subunits such as G_M (14), PP1 nuclear targeting subunit and spinophilin (15), all of which either bound poorly or failed to bind CHRM2. These results were confirmed in the current studies, which emphasized the significant decrements in CHRM2 binding to not only G_M but also neurabin and I-1.

The C-terminal residues of the PP1 catalytic subunit also contribute to the formation of a surface hydrophobic pocket that binds the RVXF motif conserved in many PP1 regulators (7). Prior studies noted that substitution of the sequence ^{290}MC^{291}, which lines the hydrophobic pocket, impaired PP1 regulation by DARPP-32 and to a much lesser extent, I-2 (15). Some PP1 regulators also displayed a remarkable selectivity for distinct PP1 isoforms. Thus, G_M selectively bound PP1β in skeletal muscle (29) and neuronal neurabin complexes primarily contained PP1γ_1 (21, 29). While the mechanism underlying PP1 isoform selectivity of regulators is not fully understood, it most likely reflects the divergent C-terminal sequences found in the different PP1 isoforms. To specifically focus on the functional analysis of the RVXF-binding pocket that is conserved in all PP1 isoforms, we undertook a limited C-terminal deletion of human PP1α to yield PP1306, which lacked the PP1α-specific sequences. PP1306 was efficiently expressed in *E. coli*, and rapidly purified using one-step affinity chromatography with MCLR-Sepharose. The purified PP1306 showed increased enzyme activity against both phosphorylase *a* and MBP when compared with PP1α. This was consistent with earlier studies, which showed that limited proteolysis of the 37-kDa PP1 catalytic subunit yielded a 35-kDa polypeptide with increased phosphorylase phosphatase activity (43). These studies suggested that the extreme C terminus of PP1α modulated its enzymatic activity.

Previous studies (44) that undertook modifications of the surface hydrophobic pocket in the single yeast PP1 catalytic subunit showed that alanine substitutions of two or more amino acids in this pocket induced lethality in yeast. Many of the "lethal" PP1 catalytic subunits, assayed as immunoprecipitates, displayed significant MBP phosphatase activity. Interestingly, yeast lethality correlated with near complete loss of

phosphorylase phosphatase activity of the mutant PP1 catalytic subunits. As regulatory subunits modify the substrate specificity of the bound PP1 (3), these data suggested the inability of mutant PP1 catalytic subunits to bind one or more regulators required for PP1-catalyzed events essential for yeast viability. To investigate the role of the hydrophobic pocket in recognition of PP1 regulators, we introduced single substitutions in the ^{289}LMC^{291} sequence that lined the RVXF-binding pocket in PP1306, substituting amino acids more commonly found in type-2 phosphatases (40). Specifically, Leu^{289} was replaced with Arg found in a plant PP2A (45), Met^{290} was substituted with Lys present in mammalian PP2A and C291 with Arg found in PP2B and several PP2A-like phosphatases. The high phosphorylase *a* and MBP phosphatase activity of all mutant PP1306 enzymes showed that these substitutions did not alter their catalytic function. This was further verified by demonstrating that the toxin sensitivity of the PP1306 mutants was similar to that of PP1α.

C291R resulted in deficits in PP1 inhibition by I-1 and Nrb (Table I and Fig. 4) comparable to those seen in CHRM2, in which 53 PP1α-specific C-terminal residues were replaced by 42 amino acids from the PP2A C terminus. In contrast, L289R and M290K had intermediate effects on PP1306 regulation by the same proteins. Direct binding analyses using either PP1 pull-down assays or overlays confirmed the critical importance of Cys^{291} in binding Nrb, I-1, and G_M. PP1 pull-down assays also showed that, whereas both L289R and M290K had modest effects on Nrb binding, M290K, and particularly L289R, were significantly impaired in their ability to bind G_M. Interestingly, in yeast (44), the substitution C290A, corresponding to human Cys^{291}, bound GAC1, the yeast homologue of G_M effectively, and accumulated WT levels of glycogen. In contrast, L288A bound GAC1 poorly, and displayed a low glycogen phenotype. Whether these differences reflect the distinct RVXF motifs present in mammalian G_M (RVSF) and yeast GAC1 (KNVRF), or the differing amino acid substitutions analyzed, remains unknown, but both L288A and C290A bound other yeast PP1 regulators, Reg1 and Sds22, like WT Glc7 (44). These data pointed to differences in the association of various PP1 regulators with the RVXF-binding pocket.

Our data highlighted three C-terminal amino acids, L288, M290, and C291, which bind the highly extended RVXF sequences (Fig. 6). Cys^{291} and Leu^{289} are particularly important, because Cys^{291} makes direct contacts with the phenylalanine that is conserved in nearly all RVXF-containing PP1-binding proteins, and Leu^{289} interacts with the valine or isoleucine also found in most PP1 regulators. Interestingly, x-ray crystallography of p53bp2, a known PP1-binding protein, suggested that the region encompassing the PP1-binding sequence, RVKF, is highly extended or linear (46), and is ideally suited for binding the surface hydrophobic pocket in a manner similar to that demonstrated by the synthetic G_M peptide (7). Cocrystallization of PP1 with the targeting subunit MYPT1 confirmed the extended nature of the KVKF sequence bound in the surface hydrophobic pocket on the PP1β catalytic subunit (9). Comparison of the flanking sequences surrounding the RVXF motifs in MYPT1 and I-1 suggested that these sequences followed distinct paths across the rear surface of the PP1 catalytic subunit to approach the catalytic site on the opposing surface and thus elicit their distinct functional effects on PP1 activity (9). Recent studies also suggested that the N- (21) and C-terminal (29) sequences flanking the RVXF motif account for the selectivity of some regulators for distinct PP1 isoforms.

To establish the critical role played by the RVXF sequence in defining the affinity of PP1 for cellular regulators, we analyzed WT GST-I-1 and the mutant GST-I-1_{RVTF} (12). The mutant I-1_{RVTF} showed a >10-fold increased binding to PP1306 (Fig. 5) and was also a 3- to 5-fold more potent inhibitor than WT I-1 (12). The identity of the RVXF motif in I-2 remains controversial, but a similar substitution of RVTF in place of the proposed PP1-binding sequence, KLHY, abolished the ability of I-2 to inhibit PP1 holoenzymes. This demonstrated that the substitution of the same RVXF motif has opposing functional effects on I-1 and I-2 and further hinted that, compared with the known RVXF-containing regulators, G_M, Nrb, and I-1, I-2 utilized a distinct mode of PP1 binding. On other hand, our previous studies (42) showed that an IKGI sequence in I-2 bound at a site adjacent to the hydrophobic pocket and, thus, I-2 binding was indirectly influenced by the substitutions L289R, M290K, and C291R. None of the pocket mutants elicited the dramatic loss in I-2 sensitivity seen in CHRM2, which was at least 200-fold less sensitive. This also provided evidence that I-2 differed from G_M, Nrb, and I-1 in its association with PP1.

The current studies demonstrated the critical role played by the surface hydrophobic pocket in PP1 association with the three cellular regulators G_M, Nrb, and I-1. They also highlighted the differing affinities of RVXF-containing PP1 regulators for the PP1α catalytic subunit, which may result from differences in the binding of distinct RVXF sequences with the surface hydrophobic pocket on the PP1 catalytic subunit. This diversity in PP1 interactions with different RVXF-containing regulators may be an important evolutionary strategy that allows further regulation of PP1 by physiological signals. Thus, the weak PP1 binding displayed by I-1, although enhanced by its phosphorylation by PKA, may be insufficient to displace more tightly bound PP1 regulatory subunits, such as G_M and Nrb, and thus in the absence of other modifications, I-1 is unable to inhibit PP1 complexes containing these regulators. In this regard, it is worth noting that PKA also phosphorylates serines within or adjacent to the RVXF motifs in G_M (47) and Nrb (48) to attenuate their association with the PP1 catalytic subunit. This in turn may facilitate the regulation of these cellular PP1 complexes by I-1 in response to hormones that elevate cAMP. Alternately, additional interactions between I-1 and regulatory subunits, such as the growth arrest and DNA damage-inducible protein GADD34 (49), may be required to circumvent the competition of these two RVXF-containing proteins for a common site on the surface of the PP1 catalytic subunit and still permit I-1 to transduce the hormonal signals that regulate the PP1/GADD34 complex and eukaryotic protein translation (41, 49). In conclusion, further studies are clearly needed to investigate the contribution of all residues that make up the RVXF-binding pocket, and thus gain a full understanding of the role of the hydrophobic pocket in the binding of cellular regulators to distinct PP1 isoforms. However, our data point to a novel experimental strategy directed at modifying or eliminating PP1 association with selected proteins and thereby elucidate the physiological role of specific PP1 complexes.

Acknowledgment—We thank Jane Richardson (Duke University) for helpful comments in creating Fig. 6.

REFERENCES

1. Ingebritsen, T. S., and Cohen, P. (1983) *Eur. J. Biochem.* **132,** 255–261
2. Ingebritsen, T. S., and Cohen, P. (1983) *Science* **221,** 331–338
3. Ceulemans, H., and Bollen, M. (2004) *Physiol. Rev.* **84,** 1–39
4. Endo, S., Zhou, X., Connor, J., Wang, B., and Shenolikar, S. (1996) *Biochemistry* **35,** 5220–5228
5. Desdouits, F., Cheetham, J. J., Huang, H. B., Kwon, Y. G., da Cruz e Silva, E. F., Denefle, P., Ehrlich, M. E., Nairn, A. C., Greengard, P., and Girault, J. A. (1995) *Biochem. Biophys. Res. Commun.* **206,** 652–658
6. Johnson, D. F., Moorhead, G., Caudwell, F. B., Cohen, P., Chen, Y. H., Chen, M. X., and Cohen, P. T. (1996) *Eur. J. Biochem.* **239,** 317–325
7. Egloff, M. P., Johnson, D. F., Moorhead, G., Cohen, P. T., Cohen, P., and Barford, D. (1997) *EMBO J.* **16,** 1876–1887
8. Baker, S. H., Frederick, D. L., Bloecher, A., and Tatchell, K. (1997) *Genetics* **145,** 615–626
9. Terrak, M., Kerff, F., Langsetmo, K., Tao, T., and Dominguez, R. (2004) *Nature*

429, 780–784
10. Liu, J., Wu, J., Oliver, C., Shenolikar, S., and Brautigan, D. L. (2000) *Biochem. J.* **346,** 77–82
11. Terry-Lorenzo, R. T., Inoue, M., Connor, J. H., Haystead, T. A., Armbruster, B. N., Gupta, R. P., Oliver, C. J., and Shenolikar, S. (2000) *J. Biol. Chem.* **275,** 2439–2446
12. Wakula, P., Beullens, M., Ceulemans, H., Stalmans, W., and Bollen, M. (2003) *J. Biol. Chem.* **278,** 18817–18823
13. Morishita, W., Connor, J. H., Xia, H., Quinlan, E. M., Shenolikar, S., and Malenka, R. C. (2001) *Neuron* **32,** 1133–1148
14. Connor, J. H., Kleeman, T., Barik, S., Honkanen, R. E., and Shenolikar, S. (1999) *J. Biol. Chem.* **274,** 22366–22372
15. Watanabe, T., Huang, H. B., Horiuchi, A., da Cruze Silva, E. F., Hsieh-Wilson, L., Allen, P. B., Shenolikar, S., Greengard, P., and Nairn, A. C. (2001) *Proc. Natl. Acad. Sci. U. S. A.* **98,** 3080–3085
16. Moorhead, G., MacKintosh, R. W., Morrice, N., Gallagher, T., and MacKintosh, C. (1994) *FEBS Lett.* **356,** 46–50
17. Walsh, A. H., Cheng, A., and Honkanen, R. E. (1997) *FEBS Lett.* **416,** 230–234
18. Zhang, A. J., Bai, G., Deans-Zirattu, S., Browner, M. F., and Lee, E. Y. (1992) *J. Biol. Chem.* **267,** 1484–1490
19. Kloeker, S., Reed, R., McConnell, J. L., Chang, D., Tran, K., Westphal, R. S., Law, B. K., Colbran, R. J., Kamoun, M., Campbell, K. S., and Wadzinski, B. E. (2003) *Protein Expr. Purif.* **31,** 19–33
20. Park, I. K., Roach, P., Bondor, J., Fox, S. P., and DePaoli-Roach, A. A. (1994) *J. Biol. Chem.* **269,** 944–954
21. Terry-Lorenzo, R. T., Carmody, L. C., Voltz, J. W., Connor, J. H., Li, S., Smith, F. D., Milgram, S. L., Colbran, R. J., and Shenolikar, S. (2002) *J. Biol. Chem.* **277,** 27716–27724
22. Connor, J. H., Quan, H., Oliver, C., and Shenolikar, S. (1998) *Methods Mol. Biol.* **93,** 41–58
23. Connor, J. H., Quan, H. N., Ramaswamy, N. T., Zhang, L., Barik, S., Zheng, J., Cannon, J. F., Lee, E. Y., and Shenolikar, S. (1998) *J. Biol. Chem.* **273,** 27716–27724
24. Sayle, R. A., and Milner-White, E. J. (1995) *Trends Biochem. Sci.* **20,** 374
25. Richardson, D. C., and Richardson, J. S. (1992) *Protein Sci.* **1,** 3–9
26. Lovell, S. C., Davis, I. W., Arendall, W. B., 3rd, de Bakker, P. I., Word, J. M., Prisant, M. G., Richardson, J. S., and Richardson, D. C. (2003) *Proteins* **50,** 437–450
27. Word, J. M., Lovell, S. C., LaBean, T. H., Taylor, H. C., Zalis, M. E., Presley, B. K., Richardson, J. S., and Richardson, D. C. (1999) *J. Mol. Biol.* **285,** 1711–1733
28. Brush, M. H., Weiser, D. C., and Shenolikar, S. (2003) *Mol. Cell. Biol.* **23,** 1292–1303
29. Carmody, L. C., Bauman, P. A., Bass, M. A., Mavila, N., DePaoli-Roach, A. A., and Colbran, R. J. (2004) *J. Biol. Chem.* **279,** 21714–21723
30. Ansai, T., Dupuy, L. C., and Barik, S. (1996) *J. Biol. Chem.* **271,** 24401–24407
31. Zhang, Z., Zhao, S., Bai, G., and Lee, E. Y. (1994) *J. Biol. Chem.* **269,** 13766–13770
32. DeGuzman, A., and Lee, E. Y. (1988) *Methods Enzymol.* **159,** 356–368
33. Campos, M., Fadden, P., Alms, G., Qian, Z., and Haystead, T. A. (1996) *J. Biol. Chem.* **271,** 28478–28484
34. Schlender, K. K., Wang, W., and Wilson, S. E. (1989) *Biochem. Biophys. Res. Commun.* **159,** 72–78
35. Goldberg, J., Huang, H. B., Kwon, Y. G., Greengard, P., Nairn, A. C., and Kuriyan, J. (1995) *Nature* **376,** 745–753
36. Kita, A., Matsunaga, S., Takai, A., Kataiwa, H., Wakimoto, T., Fusetani, N., Isobe, M., and Miki, K. (2002) *Structure (Camb.)* **10,** 715–724
37. Maynes, J. T., Bateman, K. S., Cherney, M. M., Das, A. K., Luu, H. A., Holmes, C. F., and James, M. N. (2001) *J. Biol. Chem.* **276,** 44078–44082
38. Sheppeck, J. E., 2nd, Gauss, C. M., and Chamberlin, A. R. (1997) *Bioorg. Med. Chem.* **5,** 1739–1750
39. Yang, J., Hurley, T. D., and DePaoli-Roach, A. A. (2000) *J. Biol. Chem.* **275,** 22635–22644
40. Barton, G. J., Cohen, P. T., and Barford, D. (1994) *Eur. J. Biochem.* **220,** 225–237
41. Weiser, D. C., Sikes, S., Li, S., and Shenolikar, S. (2004) *J. Biol. Chem.* **279,** 48904–48914
42. Connor, J. H., Frederick, D., Huang, H., Yang, J., Helps, N. R., Cohen, P. T., Nairn, A. C., DePaoli-Roach, A., Tatchell, K., and Shenolikar, S. (2000) *J. Biol. Chem.* **275,** 18670–18675
43. Villa-Moruzzi, E. (1986) *Arch. Biochem. Biophys.* **247,** 155–164
44. Wu, X., and Tatchell, K. (2001) *Biochemistry* **40,** 7410–7420
45. MacKintosh, R. W., Haycox, G., Hardie, D. G., and Cohen, P. T. (1990) *FEBS Lett.* **276,** 156–160
46. Gorina, S., and Pavletich, N. P. (1996) *Science* **274,** 1001–1005
47. Hubbard, M. J., and Cohen, P. (1989) *Eur. J. Biochem.* **186,** 711–716
48. McAvoy, T., Allen, P. B., Obaishi, H., Nakanishi, H., Takai, Y., Greengard, P., Nairn, A. C., and Hemmings, H. C., Jr. (1999) *Biochemistry* **38,** 12943–12949
49. Connor, J. H., Weiser, D. C., Li, S., Hallenbeck, J. M., and Shenolikar, S. (2001) *Mol. Cell. Biol.* **21,** 6841–6850
50. Higgins, D. G., and Sharp, P. M. (1988) *Gene (Amst.)* **73,** 237–244

Circulation Research

Published online before print March 3, 2005, doi:10.1161/01.RES.0000161256.85833.fa
(*Circulation Research.* 2005;96:756.)

Integrative Physiology

Enhancement of Cardiac Function and Suppression of Heart Failure Progression By Inhibition of Protein Phosphatase 1

Anand Pathak*, Federica del Monte*, Wen Zhao, Jo-El Schultz, John N. Lorenz, Ilona Bodi, Doug Weiser, Harvey Hahn, Andrew N. Carr, Faisal Syed, Nirmala Mavila, Leena Jha, Jiang Qian, Yehia Marreez, Guoli Chen, Dennis W. McGraw, E. Kevin Heist, J. Luis Guerrero, Anna A. DePaoli-Roach, Roger J. Hajjar†, Evangelia G. Kranias†

From the Departments of Pharmacology and Cell Biophysics (A.P., W.Z., J.-E.S., I.B., A.C., J.Q., G.C., E.G.K.), Molecular and Cellular Physiology (J.N.L.), Internal Medicine (H.H., F.S., D.W.M.), and Molecular Genetics and Biochemistry (L.J.), University of Cincinnati, Ohio; Cardiology Division (F.d.M., E.K.H., J.L.G., R.J.H.), Harvard Medical School and Massachusetts General Hospital, Boston, Mass; Department of Pharmacology and Cancer Biology (D.W.), Duke University Medical Center, Durham, NC; Department of Biochemistry and Molecular Biology (N.M., A.A.D.-R.), Indiana University, Indianapolis, Ind.

Correspondence to Evangelia G. Kranias, PhD, Department of Pharmacology and Cell Biophysics, University of Cincinnati, College of Medicine, 231 Albert Sabin Way, P.O. Box 670575, Cincinnati, OH 45267-0575. E-mail Litsa.Kranias@uc.edu

Abnormal calcium cycling, characteristic of experimental and human heart failure, is associated with impaired sarcoplasmic reticulum calcium uptake activity. This reflects decreases in the cAMP-pathway signaling and increases in type 1 phosphatase activity. The increased protein phosphatase 1 activity is partially due to dephosphorylation and inactivation of its inhibitor-1, promoting dephosphorylation of phospholamban and inhibition of the sarcoplasmic reticulum

calcium-pump. Indeed, cardiac-specific expression of a constitutively active inhibitor-1 results in selective enhancement of phospholamban phosphorylation and augmented cardiac contractility at the cellular and intact animal levels. Furthermore, the ß-adrenergic response is enhanced in the transgenic hearts compared with wild types. On aortic constriction, the hypercontractile cardiac function is maintained, hypertrophy is attenuated and there is no decompensation in the transgenics compared with wild-type controls. Notably, acute adenoviral gene delivery of the active inhibitor-1, completely restores function and partially reverses remodeling, including normalization of the hyperactivated p38, in the setting of pre-existing heart failure. Thus, the inhibitor 1 of the type 1 phosphatase may represent an attractive new therapeutic target.

Key Words: protein phosphatase 1 • protein phosphatase 1 inhibitor 1 • heart failure • hypertrophy • phospholamban • gene therapy

Related Article:

Targeting Protein Phosphatase 1 in Heart Failure
Hunter C. Champion
Circ. Res. 2005 96: 708-710. [Full Text]

This article has been cited by other articles:

Circulation Research ▸HOME

H. C. Champion
Targeting Protein Phosphatase 1 in Heart Failure
Circ. Res., April 15, 2005; 96(7): 708 - 710.
[Full Text] [PDF]